Geoderma 436 (2023) 116535

Contents lists available at ScienceDirect

Geoderma

journal homepage: www.elsevier.com/locate/geoderma

Water repellency by volcanic ash interacting with organic matter: Incubation response and effect on infiltration

Danny Dwi Saputra [a,b,*], Rika Ratna Sari [a,b], Indah Novita Sari [b], Didik Suprayogo [b], Meine van Noordwijk [a,c]

[a] Plant Production Systems Group, Department of Plant Sciences, Wageningen University and Research, PO Box 430, 6700 AK Wageningen, The Netherlands
[b] Department of Soil Science and Forestry, Faculty of Agriculture, Brawijaya University, 65145 Malang, Indonesia
[c] Centre for International Forestry Research and World Agroforestry (CIFOR-ICRAF), Bogor, Indonesia

ARTICLE INFO

Handling Editor: Jingyi Huang

Keywords:
Litter quality
Tephra
Hydrophobicity
Lipids
Water drop penetration time
Contact angle

ABSTRACT

Volcanic ash deposition disrupts soil surface hydrology. Our previous study showed that soil infiltration was reduced eightfold after a volcanic eruption in various land-use systems adjacent to Mount Kelud (Indonesia). Yet, soil macroporosity was relatively unchanged, indicating soil hydrophobicity. We tested the hypothesis that hydrophobicity or water repellency (WR) can be induced by volcanic ash interacting with organic matter and quantified its effect on surface water infiltration.

We combined volcanic ash with leaf litter from coffee, durian, pine and mixed sources and tested for WR as a function of incubation time (0–16 weeks) and soil water content (θ, %), with Water Drop Penetration Time (WDPT, s) and Contact Angle (CA, ^{o}) as WR metrics. Lipids content (%) and pH were also analysed during incubation. Water droplets were placed onto a material tested for WR in a slope-adjustable stage to determine the critical angle for droplet runoff before penetration. Finally, to quantify the effect of WR on water flow, we layered 5 and 10 cm of ash with organic matter additions on top of a control soil column and performed infiltration (hydraulic conductivity) measurements.

Among litter sources, pine litter induced the highest WR. There were significant relationships between WR, lipid, and pH. However, these relationships became weaker with material water contents > 7%. A significant relationship was also found between CA and critical slope of both small and large drops. A higher CA lowered the minimum critical slope for droplet runoff to 7° and 10° for the diameters of large and small water droplets, respectively. The mixture of volcanic ash and organic matter layered into the soil surface resulted in a five-times lower average hydraulic conductivity, with indications of air entrapment limiting water infiltration in a thicker ash layer. A higher CA was strongly associated with a lower hydraulic conductivity ratio, particularly under the 5 cm organic matter treatment. The WR effects on hydraulic conductivity are equivalent to at least a ten-fold reduction in effective soil porosity. By reducing infiltration, WR may contribute to ash movement in the volcanic landscape.

1. Introduction

Mature volcanic soils, Andosols, generally have high porosity, rapid infiltration of rainfall, and highly stable soil aggregates, leading to strong resistance to water-based erosion (Zehetner and Miller, 2006; Neris et al., 2012). By contrast, fresh volcanic ash (VA) is prone to soil erosion (Korup et al., 2019). Many studies documented that the deposition of volcanic materials, including tephra (lapilli and VA), hampered water infiltration and exacerbated erosion and sediment transport (Lavigne, 2004; Arnalds, 2013; Pierson and Major, 2014). VA can form encrusted strata with low hydraulic conductivity and infiltration rates on top of an older, more developed soil surface (Wilson et al., 2011;

Abbreviations: CA, Contact Angle; C_{org}, Soil Organic Carbon; CWC, Critical Water Content; K_{sat}, Saturated Hydraulic Conductivity; K_{obs}, Observed long-term Hydraulic Conductivity; K_{ref}, Reference Saturated Hydraulic Conductivity for given texture and bulk density; OM, Organic Matter; SDM, Sessile Drop Method; SWR, Soil Water Repellency; WR, Water Repellency; VA, Volcanic Ash; WDPT, Water Drop Penetration Time.

* Corresponding author at: Plant Production Systems Group, Department of Plant Sciences, Wageningen University and Research, PO Box 430, 6700 AK Wageningen, The Netherlands; Department of Soil Science and Forestry, Faculty of Agriculture, Brawijaya University, Jalan Veteran 65145, Malang, Indonesia.
E-mail addresses: dannydwi.saputra@wur.nl, danny_saputra@ub.ac.id (D.D. Saputra).

https://doi.org/10.1016/j.geoderma.2023.116535
Received 18 July 2022; Received in revised form 20 May 2023; Accepted 20 May 2023
Available online 26 May 2023
0016-7061/

Anda and Suparto, 2016). A lower hydraulic conductivity of fresh VA (Tarasenko et al., 2019) is commonly linked to the orientation of soil particles and its consequences for macropore continuity. However, the way water interacts with the surface of soil particles might also contribute to this lower hydraulic conductivity.

Soil pores provide pathways for water to infiltrate into soils. Soil infiltration can be based on soil pores that are not yet water-saturated or on typically saturated pores that pass the water onto deeper layers. Soil porosity will be high where soil texture is coarse, bulk density is low, and the soil structural development led to stable, continuous pores (Baker, 1979; Tejedor et al., 2013). Even in such conditions, however, infiltration can be slow if the soil surfaces exhibit water repellency (WR) due to hydrophobic compounds (Doerr et al., 2000). Without WR phenomena, initial infiltration rates tend to be high, as soil pores absorb water, and then gradually approach a'saturated hydraulic conductivity' dominated by the largest pore sizes, where the rate of outflow from a soil column determines the inflow rate. The presence of non-polar (hydrophobic) molecules at the soil particle surfaces, coupled with the cohesive nature of water, results in water droplets remaining intact and unable to penetrate the available pores. Additionally, air entrapment can restrict infiltration into dry soils (Wang et al., 1998; Hammecker et al., 2003; Sakaguchi et al., 2005).

VA deposition from the 2014 eruption of Mt. Kelud in East Java, Indonesia, led to soil hydrophobicity and severely inhibited infiltration (up to 8 times slower than the pre-eruption condition), despite relatively unchanged soil porosity (Saputra et al., 2022). The deposition of VA up to 20 cm in Ngantang District (Nakada et al., 2016) led to subsequent erosion and sediment transport that substantially reduced the water storage capacity of two important reservoirs in this region, Wlingi and Ledoyo, by half (Hidayat et al., 2017). This case provides an opportunity to analyze the relative roles of VA as such and VA plus organic debris as the cause of the recorded soil water repellency (SWR) in the field.

The underlying processes of WR, caused by the interactions between VA and organic matter (OM), and its consequences on soil hydraulic conductivity (infiltration), have rarely been studied compared to research conducted on other soil types or under different management practices (such as vegetation type, soil management) or fire history (Jordán et al., 2009; Jordán et al., 2011; Lucas-Borja et al., 2022). To understand the development of WR following a volcanic ash deposition, we may need to consider a sequence of events as illustrated in Fig. 1.

In the short-medium term, volcanic ash deposition may dramatically change the soil water balance through a sequence of processes (Fig. 1).

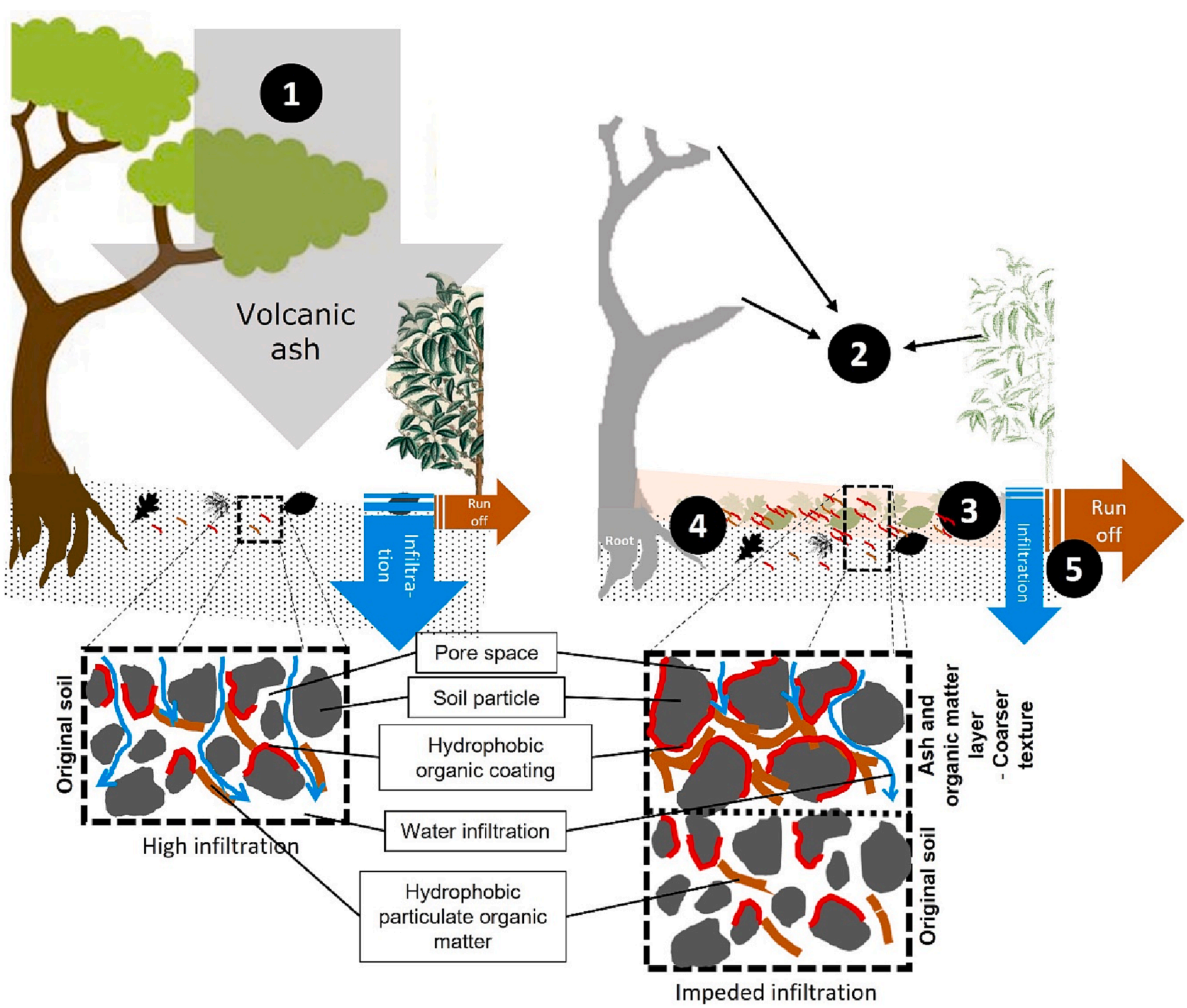

Fig. 1. Schematic process of volcanic ash deposition on an agriculture system. In the short-medium term, volcanic ash deposition may dramatically change the soil water balance through a sequence of processes: (1) volcanic eruption ejects ash materials to the atmosphere that gets deposited on agricultural land, (2) all plants may drop leaves or severely experience leaves surface abrasion (some trees survive, some die) and add a substantial amount of fresh organic matter into the soil, (3) original soil and standing litter layer may be buried under fresh volcanic ash and organic matter, (4) volcanic ash and organic matter from leaves litter and root may interact and create a water repellent surface layer, (5) soil infiltration may decrease, and on slopes, runoff and erosion occur.

Regarding steps 1, 2 and 3, the heavy load of VA deposits during a volcanic eruption may directly damage the natural and agricultural ecosystems and cause many crops and trees to partly die (Anda and Suparto, 2016; Korup et al., 2019). The soil may suddenly be loaded with a high amount of VA and plant litter, resulting in a new layer overlaying the original topsoil. This layer can lead to the development of hydrophobic material from the interaction of OM and VA. Hydrophobic substances can form a water repellent coat on VA particle surfaces (Franco et al., 2000) and a water repellent particulate OM. The type of water repellent substances produced may vary depending on the molecular composition and properties of the OM (Ellerbrock et al., 2005; Jiménez-Morillo et al., 2017; Dao et al., 2022). Lozano et al. (2013) found that lipids were one of the molecular substances strongly linked to SWR in a semi-arid Mediterranean forest. In addition, soil pH also can affect SWR by influencing soil microbial and fungi activity, which release hydrophobic substances (Doerr et al., 2006; Lozano et al., 2013). Other factors like soil-pH dependent chemical interaction may also play role in the formation of SWR (Smettem et al., 2021). In soil, pH can be influenced by the soil water content directly through the dilution of ions in the soil solution or the decrease of the solution volume due to intense evaporation. Additionally, pH can be indirectly influenced by soil water content through soil microbial activity as they release or consume acidic or basic compounds (Husson, 2013).

Regarding step 4 (Fig. 1), the inhibited soil infiltration post-volcanic eruption may be attributed to the establishment of a water repellent layer on the soil surface. The WR of this layer may be induced by the hydrophobic characteristics of VA (Berenstecher et al., 2017), and/or through hydrophobic substances derived from organic debris interacting with the VA (Poulenard et al., 2004; Kawamoto et al., 2007; Jiménez-Morillo et al., 2017). However, the relative importance of these effects remains unclear (Bachmann et al., 2000; Poulenard et al., 2004; Neris et al., 2013) and may depend on (as yet unidentified) contextual factors.

Regarding step 5 (Fig. 1), 'WR' and 'saturated hydraulic conductivity' are mutually exclusive concepts. The dependency of SWR on soil water content suggests that it is a transient phenomenon. However, while it persists, it can reduce infiltration rates and result in overland flow and erosion. Beyond the first rewetting phase, the negative impact of SWR on soil infiltration can return when the soil surface dries. In relatively dry initial soil conditions, soil pores are filled with air. Water reaching this dry soil surface cannot continue to enter soil pores if those air bubbles become trapped, especially during high-intensity rainfall (or irrigation). The combined effect of the WR layer and entrapped air bubbles within the soil matrix can have a significant impact on soil hydraulic conductivity and infiltration (Wang et al., 2000). However, the impact may still be underestimated due to the limited number of studies investigating this specific combination of factors. The topic of WR and entrapped air bubbles have been discussed separately.

This research aimed to investigate whether the establishment of WR in a mixture of VA and OM layers was correlated with the types of organic materials, and quantify the effect of WR on infiltration (hydraulic conductivity). This controlled laboratory setting experiment could help to provide evidence that the WR phenomenon generated in the lab can be related to the reduction of infiltration rate in the field. Our research questions were:

Q1A. Do the types of OM that are mixed with VA influence WR? B. Is this effect associated with lipid content and pH changes?

Q2. How does water content influence the severity and persistence of WR?

Q3. Do WR and water drop sizes influence the critical slope at which surface runoff starts? and,

Q4. How does surface-level WR relate to column-level and field measurements of infiltration rates?

2. Materials and methods

2.1. Water repellency (WR) metrics

We used two methods to evaluate WR, including (1) the Water Drop Penetration Time (WDPT) (Doerr et al., 2005), (2) the contact angle (CA) of water droplets with a Sessile Drop Method (SDM) (Leelamanie et al., 2008).

The WDPT test involves placing drops of distilled water onto the sample surface and recording the time for complete drop penetration. We put 15 g of VA sample or a mix of VA and various litter sources (see section 2.4.1) on a 90 mm diameter petri dish and levelled it with a spatula. Three water droplets were placed on the sample surface, and the actual time required for complete infiltration was recorded (de Blas et al., 2013). We took the average infiltration time values of three droplets to represent the sample.

We also measured the CA of water droplets. The sample particles were sprinkled on a double-sided tape (1.5 cm × 1.5 cm) pasted onto a smooth surface of a 90 mm diameter of petri dish. The particles adhering to the tape were pressed using a 100-gram load for 10 s to get a thin one-grain sample layer with a similar diameter. The sample layer was then gently tapped to remove surplus soil particles from the sample. The procedure was repeated twice. After preparation, the samples were placed on a stage in front of a digital camera, as illustrated in SI.1. Three droplets of 10 μL distilled water were sequentially placed onto an unaffected (from the previous drop) part of the sample surface using a pipette. A digital photograph of the horizontal view of each water droplet was taken within one second (Leelamanie et al., 2008). The CA of both sides of each water droplet was determined by analysing the photograph images using ImageJ apps with drop-analysis plug-ins (Stadler and Sage, 2020). The mean CA value from both sides of the water droplets was used for further analysis. A sample was classified as hydrophobic if CA was $>90^{\circ}$ (Simpson et al., 2015).

2.2. The effect of WR on the relationship between critical slope and runoff

As a novel, additional method, a simple procedure was designed to test the relationships between the slope and runoff of droplets before infiltration. To generate the slope dataset, we placed samples of different WR levels (CA $> 90^{\circ}$) inside a petri dish on an adjustable stage (sturdy handphone holder) to set the slope (SI.2). We placed a droplet of distilled water into the sample, quickly took a photograph for CA measurement, and adjusted the gradient to a point where the droplet started to slide down (representing the soil runoff occurrence). This procedure took approximately 5 s. Slope adjustments immediately made after the water droplets were applied to the WR surface may allow for movements and energy changes that may impact the infiltration process. Nevertheless, such effects may only marginally change the runoff initiation with the increasing slope. The diameter of drop sizes is crucial for this experiment. Here, we used two different water drop diameters of small (2.8 mm) and large (8.5 mm), as it represents the range of raindrop diameter sizes in tropical regions, as reported by Yakubu et al. (2016).

2.3. Volcanic ash (VA) collection and preparation

We used VA materials from the 2014 Mt. Kelud eruption deposited in Sumberagung Village, Ngantang District, East Java, Indonesia. VA term refers to the pyroclastic materials deposition of < 2 mm tephra fractions (Arnalds, 2013; Rossi et al., 2021). Farmers collected the VA approximately two months after the eruption. VA was stored in a dry condition and has not been modified by the interaction with the existing vegetation in the landscape. Saputra et al. (2022) reported that the VA has material distribution sizes of 81%, 14%, and 5% sand-, silt-, and clay-size particles, respectively. VA also had a very low soil organic carbon content (C_{org}) of < 0.01%.

VA was sieved using a 2 mm mesh sieve. To dry the VA, we heated the sample to a temperature of 200 °C for 60 min using a muffle furnace. In the preliminary experiment (SI.3), VA exhibited a hydrophobic state (CA > 90°) after the heating process. However, it was observed that the VA returned to a hydrophilic state in<48 h. This particular high-temperature treatment was within the estimated temperature range of volcanic ash flow from the Merapi eruption in Indonesia (<300 °C) inside the radial distance of 9–16 km from the vent (Jenkins et al., 2013). Similarly, Pensa et al. (2019) estimated volcanic ash temperature in an unconfined distal area up to 8–10.5 km from the crater as in 170°-220 °C range during the Volcan de Colima eruption (Mexico). The dried VA was stored at laboratory conditions (temperature between 23 and 25 °C with an average relative air humidity of 65%) for two days before further being used for laboratory analyses and experimental materials.

2.4. Experiments setup

2.4.1. First experiment: The effect of different organic matter (OM) sources on WR indicators

To answer Q1, we designed an experiment with three different plant litter sources and one mixture litter to represent the range of OM expected in the agroforestry landscapes affected by Mt. Kelud ash. The OM sources include litter from *Coffea canephora* (Robusta coffee), *Durio zibethinus* (Durian), *Pinus merkusii* (Pine) and mixed litter of *C. canephora, D. zibethinus* and *P. merkusii*. The experiment included five treatments: (1) volcanic ash (VA), (2) VA + *C. canephora*, (3) VA + *D. zibethinus*, (4) VA + *P. merkusii*, and (5) VA + mixed.

Litter from *C. canephora, D. zibethinus* and *P. merkusii* were classified as high, medium, and low litter quality, respectively (Purwanto et al., 2007; Chae et al., 2019; Ishaq et al., 2020). High litter quality has a low C:N ratio and lignin plus polyphenol to N ratio, (L + Pp)/N, and decomposes rapidly (Sari et al., 2022). We gathered freshly abscised leaf litter from agroforestry plots, at the same place where we collected the ash materials. The litter was air-dried for 48 h and ground. The ground litter was then sieved using a 2 mm mesh sieve and stored under laboratory conditions before further chemical analysis. We used ≤ 2 mm of particle size as it induced the highest CA compared to larger OM particle size treatments (SI. 4), representing the maximum-potential level of WR that OM could produce. Furthermore, ≤2 mm also represents the size of decomposed organic materials when they turn into soil organic matter.

VA and litter were mixed to achieve a 16% OM proportion. This OM proportion was based on the third preliminary experiment (SI.5) that tested a wider range of VA to OM ratios for the degree of WR induced. This high OM proportion is realistic for the top few cm of mixed VA + OM layer formed after the volcanic eruption. During the volcanic eruption, VA precipitation induces significant defoliation and abrasion of leaves and other tree components (biomass) and buries all of the standing litter (necromass).

The mixing of VA and litter of each treatment was performed manually in large quantities. For each replication, around 30 g of material were incubated in small aliquots, with one for each time step. To maintain a constant water content, each aliquot was placed in a sealed plastic bag. Before measuring WR, the material in each aliquot was homogenized. The WDPT and CA were measured initially and after five time steps (0, 1, 2, 4, 8, 16 weeks) to understand the longevity/persistence of WR for each treatment and its correlation with extractable lipids content and soil pH (for further explanation on lipids and pH analysis, please see Section 2.5). Each treatment was replicated four times for a total of 120 samples. However, for CA and WDPT, a total of 360 data points were recorded, as we measured each sample three times (please see Section 2.1).

2.4.2. Second experiment: The effect of soil water content on WR

We designed the second experiment to determine the WR sample's critical water content (CWC) and transition zone (**Q2**). The VA + *P. merkusii* material from the first experiment was used, as this treatment induced the highest WR. CWC refers to the water content at which the effect of WR on the material is no longer present. Various amounts of water were added to the sample to create different water contents (θ, %). Samples were carefully mixed, put inside a sealed plastic bag, and left for a day to equilibrate before the first measurement. The actual water content was determined gravimetrically before measuring CA and WDPT. Five different water content treatments, including < 4%, 4–7%, 7–10%, and > 10%, were used in this experiment. The persistence of WR was studied by conducting measurements at five different times after the start of the experiment (0, 1, 2, 4, 8, 16 weeks). All treatments were replicated four times, for a total of 96 samples.

2.4.3. Third experiment: The critical slope–runoff relationship affected by WR

The third experiment was designed to study the relationships between WR (represented by CA) and the critical (minimum) slope at which water droplets started to run off (**Q3**). VA + *P. merkusii* material with varying water content to create a range of CA. To achieve different CA, we conditioned the samples by adding 0.25 ml, 0.5 ml, and 1 ml of water into each sample unit. After homogenizing and incubating the samples for one day, we measured the actual water content gravimetrically. The actual water content ranged from 1 to 1.6%, 2–2.6%, 4.1–5.2% for the 0.25, 0.5, and 1 ml water additions, respectively. This procedure produced CA values ranging from 95° to 153°. We replicated all treatments five times. For detailed WR measurement procedures please see section SI.2.

2.4.4. Fourth experiment: The effect of WR as a surface layer property on soil infiltration and hydraulic conductivity

The fourth experiment aimed to assess the impact of VA and OM layer on infiltration (hydraulic conductivity) (**Q4**). For this purpose, six treatments were applied, including (1) original soil 'as a control', (2) original soil + VA, (3) original soil + VA + *C. canephora*, (4) original soil + VA + *D. zibethinus*, (5) original soil + VA + *P. merkusii*, and (6) original soil + VA + mixed litter. The 'original' soil column used in the experiment was obtained from the topsoil of coffee-based agroforestry systems and had the following characteristics: loam texture with 16% clay, 37% silt, and 50.8% sand, a bulk density of 0.99 g cm^{-3} and C_{org} content of 1.1%. Two different treatments of 5 and 10 cm depth of water repellent material layer were added to the original soil column before conducting the infiltration (hydraulic conductivity) measurement. These values represent the range of deposited volcanic ash thickness measured near Mt. Kelud after the 2014 eruption (Saputra et al., 2022). We tried to recreate the field condition post volcanic eruption where our field-measured steady state infiltration rate was dramatically drop compared the pre-eruption. The treatments were replicated four times. All experiments (1–4) were performed under a climate-controlled laboratory setting at an air temperature ranging from 23 to 25 °C and an average relative air humidity of 65%.

Soil hydraulic conductivity was assessed using a 'falling' head method in a laboratory setting (Novák et al., 2009). The undisturbed soil column samples were collected using a plastic cylinder with a volume of 238 cm^3 (diameter 5.5 cm) at the same location where the VA and litter were taken. The field-collected soil column samples were saturated using tap water from the sample bottom to allow the air to escape for 48 h. We applied a 5 or 10 cm layer of dry water repellent material on top of the original soil column and then added water to the soil column until the water level reached 23 cm above the sample surface. We measured the difference between the first and second water level reading at 1-minute interval. If the water level reduced to around 15 cm above the sample surface, we readjusted it back by adding additional water. This process was repeated for a total observation time of 2 h. This procedure was applied for all measurements.

We expected to observe the common infiltration pattern in water repellent material, where the initial low infiltration rate would increase over time as the material became more wettable. However, our data did not show this pattern. Within two hours of observation time, the infiltration rate declined from the initially high to a lower rate. Therefore, to estimate the initial infiltration rate as well as the steady state infiltration rate, which is equal to hydraulic conductivity, we used the standard Horton equation (Horton, 1941; Mahapatra et al., 2020). The estimation was done by curve fitting of Horton's equation using SigmaPlot 10 software (Saputra et al., 2020) as follows:

$$f_p = f_{min} + (f_{max} - f_{min})e^{-k_d t} \tag{1}$$

where:

f_p: infiltration rate at time t, cm h^{-1}.
f_{max}: initial infiltration capacity or maximum infiltration rate, cm h^{-1}.
f_{min}: (quasi)-steady state infiltration rate representing hydraulic conductivity, cm h^{-1}.
k_d: exponential decay constant specific to soil, $time^{-1}$.

The equation predicts a smooth decline from the initially high infiltration rate, when water can fill air-filled pore spaces, to the rate at which it can be passed, supposedly indefinitely, through the whole column once this is saturated and the largest pore sizes dominate the result. As an alternative to analysis of the temporal change in f_p, the rates were also compared to the RelCumInf parameter that divides the cumulative infiltration by the total pore space in the soil column (whether air-filled or water-filled at the start of the measurements).

In standard theory the f_{min} parameter in equation (1) represents K_{sat} or saturated hydraulic conductivity. In our case, there were doubts that the soil was completely water-saturated towards the end of the measurement periods. Faybishenko (1995) refers to this term as quasi-saturated hydraulic conductivity to describe the state in which air is trapped in soil but not connected to the atmosphere. We refer to the f_{min} or quasi-saturated hydraulic conductivity parameter simply as K_{obs}, the observed hydraulic conductivity.

We compared this K_{obs}, derived as the f_{min} parameter in Eq. (1), to what the van Genuchten (Hodnett and Tomasella, 2002) pedotransfer function (hydraulic conductivity = f(texture, macroporosity)) predicts for a soil with the same texture and bulk density (K_{ref}). However, as the predicted hydraulic conductivity values from the van Genuchten pedotransfer function were higher than our lab measurements for the original soil, we used the ratio between the two values rather than directly used the predicted values.

Furthermore, a 'relative equivalent porosity' term was defined as the relative macroporosity for which the reference soil (in the van Genuchten pedotransfer function) would yield the observed K_{sat}. We used a log10 transform to interpolate between the tabulated points generated from the van Genuchten pedotransfer function. Hydraulic conductivity ratio (K ratio) in equation (2) and relative equivalent porosity in equation (3) were used to test the consequence of WR (represented by CA) as a surface property on soil column hydraulic conductivity (**Q4**).

$$K\ ratio = K_{obs}/K_{ref} \tag{2}$$

where:

K_{obs}: observed hydraulic conductivity.
K_{ref}: reference hydraulic conductivity.

$$Relative\ equivalent\ porosity = \Phi_{ref}/\Phi_{obs} \tag{3}$$

where:

Φ_{ref}: reference macroporosity.
Φ_{obs}: observed macroporosity.

2.5. Physico-chemical analysis

Physico-chemical analysis of VA was performed at the Soil Science and Forestry Department laboratory of Brawijaya University. The soil organic carbon (C_{org}) content was measured using the wet oxidation of Walkley and Black method (Anderson and Ingram, 1994). This method involves the oxidation of OM by potassium dichromate ($K_2Cr_2O_7$) with sulfuric acid (H_2SO_4) to heat the dilution, followed by colorimetric titration. Soil texture was determined using the pipette method (Bieganowski and Ryżak, 2011). The pH of the soil–water mixture (1:5 ratio) was measured using an electrodes-connected pH meter.

Extractable lipids

The extractable lipids content of 120 samples was analysed with the Soxhlet method (Perera and Brown, 1996) in the Food Technology Laboratory of Universitas Muhammadiyah Malang. Lipids content from a 2 g freeze-dried sample was extracted with 20 ml of petroleum ether solvent using Soxhlet apparatus for six hours. Extracts were filtered and dried (evaporated) at 40 °C for about 30 min until no solvent was seen and were kept in a desiccator at room temperature before weighing. Total lipids content was gravimetrically determined and expressed as percentages of the dry sample weight (Helrich, 1990).

2.6. Data analysis

The main and interactive effects of treatments of WR (expressed by CA and log WDPT), pH, lipids content, and K_{obs} were analysed using two-way ANOVA after evaluating the data normality by checking the skewness and kurtosis metrics. The WDPT data (experiments 1 and 2) were log-transformed, while the CA (experiment 1) and lipids (experiment 2) were square root-transformed prior to analysis to meet the normality assumption. The non-transformed data were used for data presentation in figures and tables, except for WDPT. Statistical differences were considered significant at $p \leq 0.05$ level. Pairwise differences were tested using Tukey's HSD *post-hoc* test. We fitted a logarithmic regression model to address the relationships between CA and log WDPT with lipids, and a linear regression model between CA and log WDPT with pH (**Q1** and **Q2**). The relationships between CA with the critical slope for runoff (**Q3**), and CA with K_{sat} ratio and relative equivalent porosity (**Q4**) were fitted using a simple linear regression model. We performed all statistical analyses using R 4.1.2 (R Core Team, 2021).

3. Results

3.1. The effect of different organic matter types on lipids, pH, and WR indicators

The incubation time had a strong effect on the CA and log WDPT of the water-repellent material, with the concentration of lipids as a potential causal factor. Additionally, the pH difference between samples with and without litter gradually increased over time (Fig. 2). Exponential decay functions were used to model the difference between VA and VA + litter, and they provided a good fit for the data. The effect on CA, log WDPT and lipids decreased 1.5, 0.8 and 4.6% per week, respectively.

Lipids content was zero for the VA samples and 2.4% on average for the VA + litter samples, without statistically significant difference between the litter sources, but a substantial decline over time (SI. 6). A substantial decrease in lipids was found during the first week of incubation time, with an average reduction of 23% relative to the initial value. The most significant reduction was found in VA + mixed OM treatment (28%) during this first week, followed by VA + *P. merkusii*, VA + *D. zibethinus,* and VA + *C. canephora* with 26%, 22%, and 17%, respectively. Whereas, between weeks 2 to 16, we identified a slow and steady lipids reduction in all VA + OM treatments with an average relative decline of 2.2% per week.

The pH differed significantly among the treatments. In general, OM

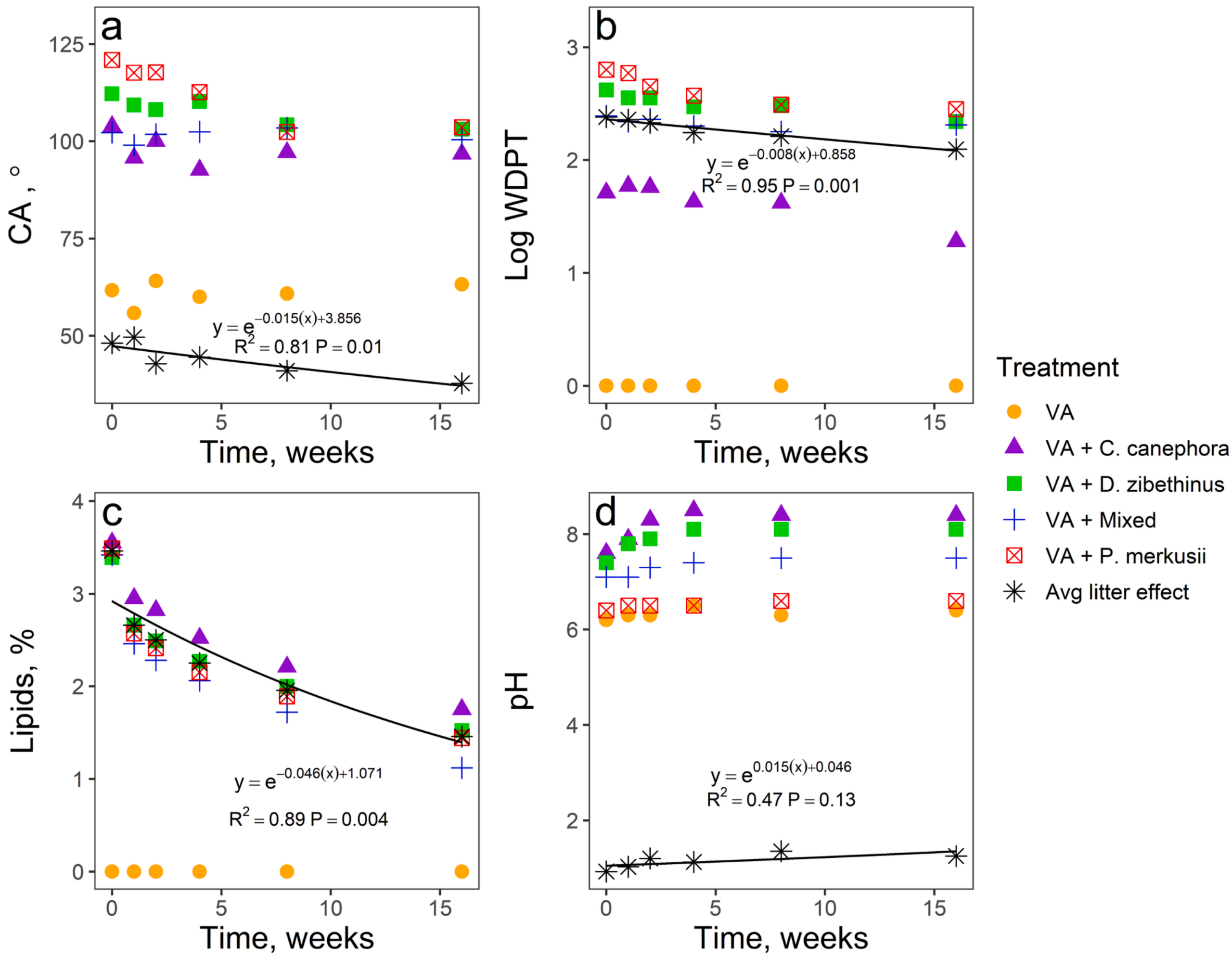

Fig. 2. The measured (a) CA, (b) log WDPT, (c) lipids content and (d) pH of water repellent materials during a 16-week incubation in experiment 1. The average litter effect (Avg. litter effect) was calculated by subtracting the control treatment (VA) from the average value of all litter treatments. The average litter effect was fitted using an exponential regression model. CA: Contact Angle, WPDT: Water Drop Penetration Time, WR: Water Repellency, VA: Volcanic Ash.

addition to VA increased pH. The VA + *C. canephora* treatment increased pH by nearly two units compared to only VA. Whereas, the VA + *P. merkusii* elevated the pH by 0.2, the lowest among other treatments. There was a tendency for pH to increase with observation periods. However, significant increases were only found for VA + *C. canephora*, VA + *D. zibethinus*, and VA + mixed OM treatments.

The mix of VA and various OM sources induced WR showed by its CA and log WDPT values (SI. 6). VA + OM treatments increased CA to > 90° (indicating hydrophobicity). VA + *P. merkusii* treatment had the highest average of CA (112°), followed by VA + *D. zibethinus*, VA + *C. canephora*, and VA + mixed OM (108°, 99.6° and 97.6°, respectively). The increases of CA values followed by a more extended time needed for the water droplets to infiltrate into the sample, as shown by a higher log WDPT (SI. 7). The time range required for a water droplet to penetrate the VA and OM samples was between 17 and 755 s, corresponding to slight to severe WR based on the classification of Bisdom et al. (1993). The highest average of log WDPT was found in VA + *P. merkusii*, VA + *D. zibethinus*, VA + mixed (strong WR level), followed by VA + *C. canephora* (slight WR level). In contrast, the water droplets were instantly infiltrated into the sample for the VA treatment, with an average CA of 61°.

During the 16-weeks observation period, all treatments involving a combination of VA and OM showed WR (CA > 90°). The persistence of CA varied significantly among treatments. The treatment of VA + mixed litter exhibited the slowest decline in CA (-0.4 % per week), while VA + *P. merkusii* showed the fastest decline (−2.6 % per week). The other two litter sources showed a decline similar to the overall average (-1.5 % per week). In contrast, VA and VA + mixed litter showed constant CA throughout the 16-weeks period.

3.2. *The effect of different water contents on lipids, pH, and WR (CA and log WDPT)*

We used the VA + *P. merkusii* treatment sample (which had the highest WR), to analyse the effect of soil water content on lipids, pH and WR indicators, and their temporal change (second experiment). The decline of lipids within the observation period was slowest for the driest soil treatment (Table 1). The average lipids content across the observation times at < 4% water content treatment was 1.4, 2.0, and 2.4 times higher than that found in the 4–7, 7–10, and > 10% treatments, respectively.

The decay of lipids was 3.8, 10, 17 and 22% per week, while pH increased by 2.33, 1.94, 2.36, and 6.62% per week for soils kept at a water content of < 4%, 4–7%, 7–10% and > 10%, respectively. The CA difference between the average control treatment (VA) in experiment 1 and the average of organic matter addition treatments in experiment 2 (ΔCA) decreased by 2.2, 2.5, and 3.5% per week for water content < 4%, 4–7%, and > 10%, respectively. However, we found a slight increase (0.43% per week) of 7–10% water content. It should be noted that at soil water contents > 7%, the initial ΔCA was already small. The log WDPT decreased by 2.4, 0.9% per week for water content < 4% and 4–7%, but

Table 1
The observed lipids, pH, contact angle, and log water drop penetration time (Log WDPT) of the mixed VA + *P merkusii* material from four different water content treatments of < 4%, 4–7%, 7–10%, and > 10%.

Treatments	Weeks	Lipids, %	pH	Contact angle, °	Log WDPT, s
<4%	0	3.49 ± 0.08^{n}	6.40 ± 0.04^{a}	126.6 ± 2.9^{hi}	2.9 ± 0.01^{e}
<4%	1	2.53 ± 0.02^{m}	6.35 ± 0.05^{a}	120.3 ± 1.3^{ghi}	2.7 ± 0.02^{cde}
<4%	2	2.24 ± 0.07^{lm}	6.65 ± 0.03^{bcd}	115.4 ± 2.7^{fgh}	2.6 ± 0.04^{cd}
<4%	4	2.02 ± 0.06^{klm}	6.68 ± 0.03^{bcde}	108.4 ± 2.3^{defg}	2.6 ± 0.04^{cd}
<4%	8	1.83 ± 0.07^{jkl}	6.68 ± 0.06^{bcde}	107.3 ± 0.5^{cdef}	2.5 ± 0.05^{c}
<4%	16	1.58 ± 0.06^{ijk}	6.80 ± 0.00^{defghi}	104.4 ± 0.9^{bcdef}	2.4 ± 0.02^{c}
Av. < 4%		2.28 ± 0.13^{C}	6.59 ± 0.04^{A}	113.7 ± 1.8^{C}	2.61 ± 0.03^{C}
4–7%	0	3.49 ± 0.08^{n}	6.59 ± 0.01^{bc}	128.7 ± 4.0^{i}	2.8 ± 0.07d^{e}
4–7%	1	2.24 ± 0.10^{lm}	6.71 ± 0.03^{cdef}	112.2 ± 2.3^{efg}	2.7 ± 0.06^{cde}
4–7%	2	1.25 ± 0.12^{hij}	6.83 ± 0.03^{defghi}	109.8 ± 1.9^{efg}	2.7 ± 0.07^{cde}
4–7%	4	1.10 ± 0.12^{ghi}	6.89 ± 0.02^{fghij}	107.4 ± 1.7^{cdef}	2.6 ± 0.06^{cd}
4–7%	8	0.88 ± 0.13^{fgh}	6.91 ± 0.03^{ghi}	100.6 ± 1.4^{bcde}	2.6 ± 0.04^{cd}
4–7%	16	0.48 ± 0.15^{cde}	6.98 ± 0.05^{hi}	100.7 ± 1.2^{bcde}	2.6 ± 0.05^{cd}
Av. 4–7%		1.57 ± 0.21^{BC}	6.8 ± 0.03^{B}	109.9 ± 2.1^{C}	2.7 ± 0.03^{C}
7–10%	0	3.49 ± 0.08^{n}	6.51 ± 0.02^{ab}	94.5 ± 4.3^{b}	1.5 ± 0.23^{b}
7–10%	1	1.76 ± 0.04^{jkl}	6.75 ± 0.02^{cdefgh}	92.4 ± 4.3^{b}	1.5 ± 0.21^{b}
7–10%	2	0.74 ± 0.05^{efg}	6.91 ± 0.04^{ghi}	95.2 ± 1.3^{bc}	1.5 ± 0.15^{b}
7–10%	4	0.57 ± 0.06^{def}	6.85 ± 0.02^{efghi}	95.5 ± 0.9^{bc}	1.6 ± 0.12^{b}
7–10%	8	0.29 ± 0.07^{bcd}	6.93 ± 0.01^{ghi}	94.7 ± 2.5^{b}	1.6 ± 0.11^{b}
7–10%	16	0.14 ± 0.04^{ab}	7.04 ± 0.02^{i}	96.4 ± 0.8^{bcd}	1.6 ± 0.13^{b}
Av. 7–10%		1.16 ± 0.24^{AB}	6.8 ± 0.04^{B}	94.8 ± 1.0^{B}	1.5 ± 0.06^{B}
>10%	0	3.49 ± 0.08^{n}	6.50 ± 0.04^{ab}	70.1 ± 3.8^{a}	0.2 ± 0.02^{a}
>10%	1	1.32 ± 0.14^{hij}	6.83 ± 0.02^{defghi}	68.8 ± 2.5^{a}	0.2 ± 0.03^{a}
>10%	2	0.55 ± 0.07^{def}	6.72 ± 0.07^{cdefg}	68.0 ± 1.1^{a}	0.1 ± 0.03^{a}
>10%	4	0.19 ± 0.03^{abc}	6.89 ± 0.02^{fghi}	72.4 ± 1.3^{a}	0.2 ± 0.03^{a}
>10%	8	0.09 ± 0.02^{ab}	7.49 ± 0.01^{j}	65.9 ± 1.3^{a}	0.1 ± 0.02^{a}
>10%	16	0.06 ± 0.01^{a}	7.58 ± 0.03^{j}	66.2 ± 0.8^{a}	0.2 ± 0.02^{a}
Av. > 10%		0.95 ± 0.25^{A}	7.0 ± 0.08^{B}	68.6 ± 0.9^{A}	0.17 ± 0.01^{A}

Note: Av. = average value of each treatment; the values displayed are means ± standard error (SE); the interaction between treatments with incubation time is represented by the lowercase letter following the values in each treatment; the difference between treatments is represented by the uppercase letter following the average value in each treatment (in bold); different letters within a variable are significantly different at P < 0.05.

slightly increased by 0.69 and 0.01% per week for water content 7–10% and > 10%, respectively, again with a small initial effect size at soil water contents > 7%.

The critical water content (CWC) for WR to be noticeable in the VA + *P. merkusii* treatment was 10% (v/v). The samples with CA < 90° in the > 10% water content treatment exhibited a short WDPT. However, the average log WDPT of 0.17 was classified as wettable based on the Bisdom et al. (1993) WR rating.

Interaction between water content and observation periods on CA among the treatments was only significant for water content < 7%, with a decreased tendency along with the time observations (Table 1). Meanwhile, for the log WDPT, that interaction was substantial for water content < 4%. The CA difference between hydrophobic samples (<4%, 4–7%, and 7–10% treatments) became marginal at the end of the observation time. The consistently significant differences in log WDPT along the observation periods were found between samples with < 7% water content. The Bisdom et al. (1993) WR ratings were wettable (>10%), slight (7–10%), and strong (4–7 and < 4%) with the average log WDPT of 0.17, 1.5, and 2.65, respectively.

3.3. The relationships between lipids content, pH and WR indicators from the different OM treatments

Although the various parameters exhibited different patterns of change with incubation time, significant relationships were found across different observation times between CA and log WDPT with lipids (Fig. 3). Within litter treatments, the most significant relationship between WR (CA and log WDPT) and lipids was found in VA + P. *merkusii* (SI.8). An increase in lipids content beyond 1% associated with a marginal increase in WR. Interestingly, although similar lipids content was found between VA + *C. canephora* and other OM treatments, the log WDPT in this treatment was noticeably lower, indicating that other factors beyond those measured may also contribute to WR development. Additionally, a reduced WR was noted with increased pH, as shown in Fig. 3.

3.4. The relationships between lipids, pH, and WR indicators from the different water content treatments

We found that lipids content was positively associated with WR, while pH was otherwise (Fig. 4). WR represented by CA was more closely correlated to lipids and pH changes than log WDPT. However, our data demonstrate that WR changes were substantially controlled by water content treatments rather than lipids and pH. This tendency was indicated by the development of data clusters that refers to the water content treatments, particularly noticed in the > 7% water content treatments. However, lipids and pH in drier materials were highly related to CA and Log WDPT (SI. 8).

3.5. The relationship between CA and critical slope for runoff

CA was negatively related to the critical slope when runoff starts. However, the relationships differed with droplet size (Fig. 5 and SI.8). A lower critical slope was required for immediate runoff in a large raindrop diameter (range of 7-16° critical slope) than the small diameter (range of 10–45° critical slope) within the WR treatments.

3.6. The effect of WR surface layer on infiltration and observed hydraulic conductivity (K_{obs})

The initial infiltration rates were well correlated with the quasi-steady state infiltration (Fig. 6), with an intercept that reflects more than proportional reductions of f_{min} relative to f_{max} in soils with low overall infiltration rates. Although the Horton equation used to estimate the K_{obs} values produced acceptable fits (Fig. 7), the change with time in the observed infiltration rate in the volcanic ash soils differed from the

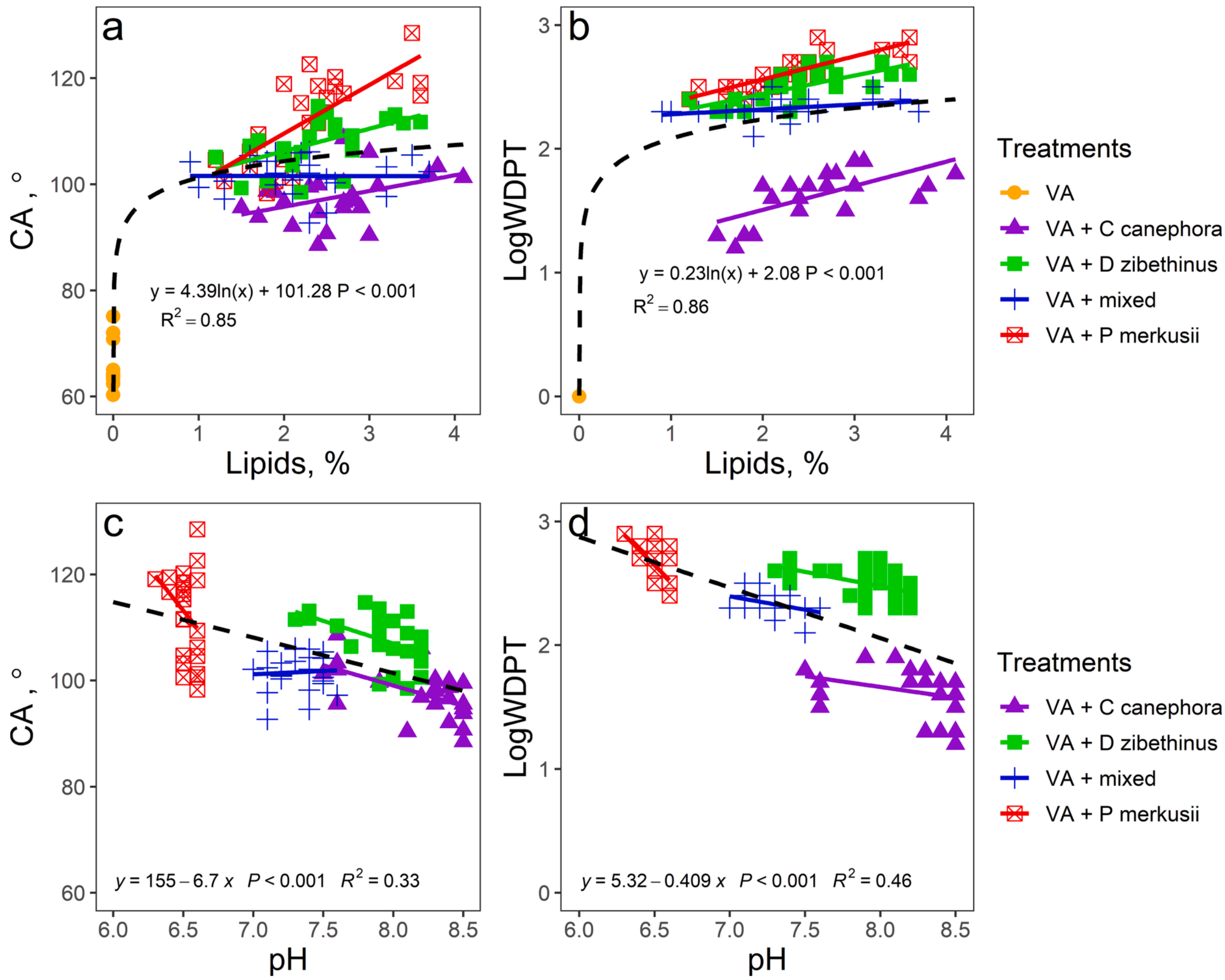

Fig. 3. The relationships between lipids content and (a) CA, (b) log WDPT; and between pH and (c) CA and (d) log WDPT under VA and different organic matter sources treatments. We excluded VA dataset for the pH and WR indicators (CA and log WDPT) regression analyses. CA: Contact Angle, WDPT: Water Drop Penetration Time, VA: Volcanic Ash.

gradual approach to a K_{obs} that can be sustained for as long as measurements would be continued. Instead, the VA + organic sources showed a continuously declining infiltration rate, with the most substantial effect seen in the 10 cm layer of VA + *P. merkusii*. When the infiltration rate was related to the RelCumInf parameter, results indicated that K_{obs} was obtained after the total soil pore volume had been many times (10 – 100 times) replaced, indicating a strong preferential flow (as opposed to 'piston flow').

The K_{obs} values generated from the Horton equation were log-normally distributed, with the value range of 6–131 cm h^{-1}. Overall, the added layer treatments significantly reduced K_{obs} by an average of 79% (24 cm h^{-1}), or five times lower than the reference soil (112 cm h^{-1}) (Fig. 8). Relative to control soil, VA and OM treatments reduced the averages of K_{obs} by 71 and 87% for 5 and 10 cm layer thickness, respectively. The addition of various OM as hydrophobic materials further hampered K_{obs} by an average of 45% (5 cm layer) and 25% (10 cm layer) relative to VA treatments. The highest K_{obs} reduction was observed for the combination of VA + *P. merkusii*, almost 19 times lower than the reference soil. Similar to K_{obs}, we found that the initial infiltration (initial rate of water flows into the WR layer + soil column) was significantly different between the control and treated soil columns. Adding VA and various OM sources to the original soil column surface reduced the averaged initial infiltration rate from 143 cm h^{-1} to 52 cm h^{-1}. Even though we found no significant difference in the infiltration rate decay constant or -*k* among treatments (SI. 9 a and b), we identified that WR metrics (CA and log WDPT) have a negative relation to -*k* (SI. 10a and b).

We found strong negative relationships between K ratio and relative equivalent porosity with CA in 5 and 10 cm layers of VA and VA + OM treatments (Fig. 9). However, the lower regression line gradient of 10 cm layer thickness compared to 5 cm treatment indicates that the influence of WR on K ratio and relative equivalent porosity reduction became less substantial with thicker volcanic ash and organic matter layer added.

4. Discussion

The experiments showed that the types of OM mixed with VA influence WR (**Q1A**). However, a direct attribution to lipids content and pH changes could not be made, as the temporal dynamics differed between parameters (**Q1B**). We also found that soil water content influences the severity and persistency of WR, with a critical soil water content of 10% above which WR effects are negligible (**Q2**). WR and droplet diameter size influenced the critical slope at which drops of water will runoff before they infiltrate (**Q3**). Finally, we found that the column-level soil infiltration and hydraulic conductivity was affected by surface-level WR (**Q4**).

In matching our process-level laboratory results to the field conditions, a number of steps in the experimental procedure need to be taken

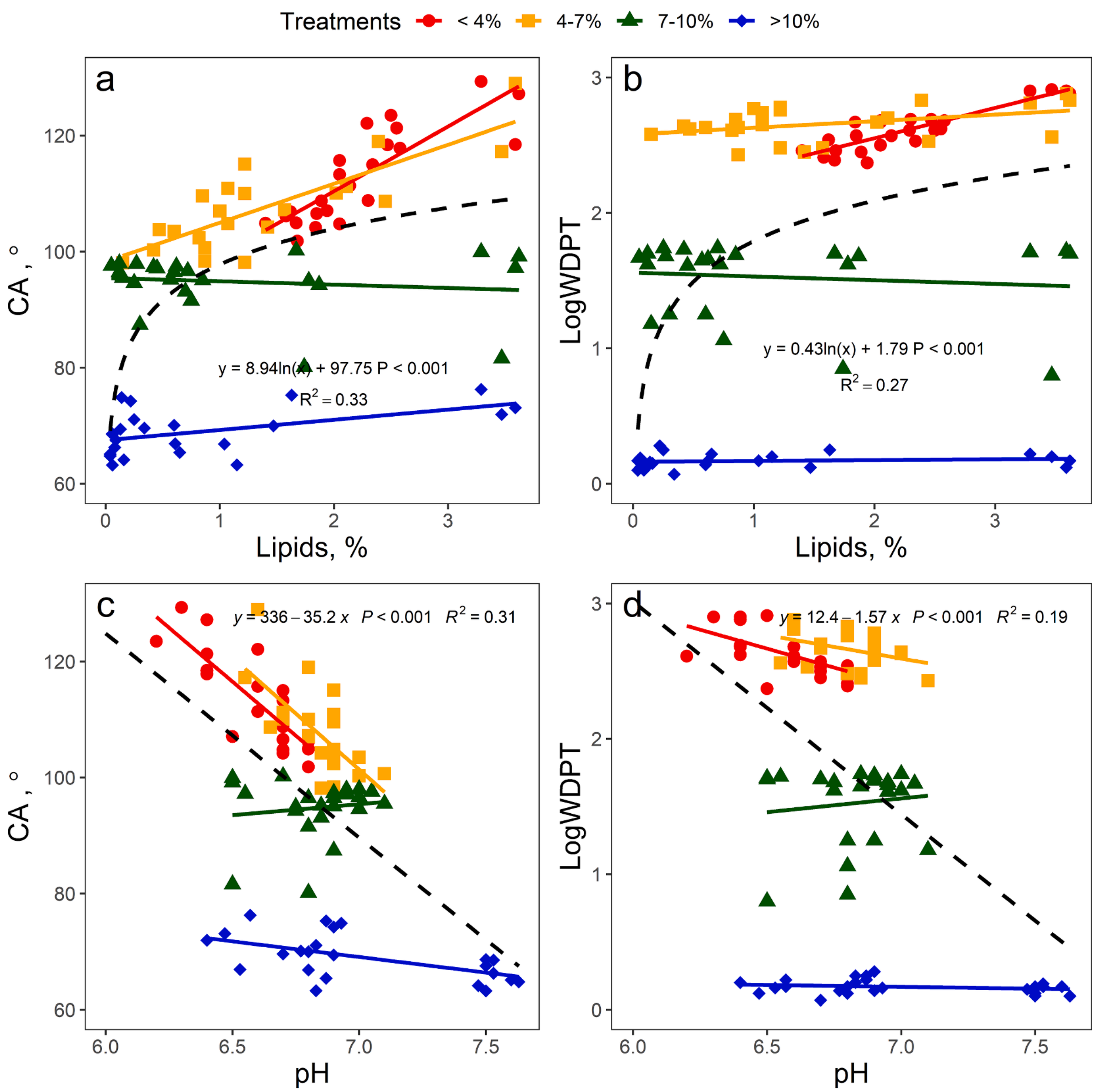

Fig. 4. The relationships between lipids content and (a) CA, (b) log WDPT; and between pH and (c) CA and (d) log WDPT under different water content treatments. CA: Contact Angle, WDPT: Water Drop Penetration Time.

into account, such as the homogenization of litter material. We used ground fresh litter material, as this type of OM was probably predominant in the newly deposited volcanic ash, but we did not explore the effects of litter particle sizes, and litter to ash ratios beyond the preliminary experiment (SI. 4 and 5).

Q1: Difference litter sources induced a different level of WR through their lipids content and pH modification

The addition of litter to volcanic ash induced WR. However, the severity of WR depended on the litter source. We found that the litter from *P. merkusii* induced the highest severity of WR compared to other litter treatments, with a CA of 112° and log WDPT of 2.62. Our results are similar to those of Neris et al. (2013), who found that the pine forest floor in Tenerife (Canary Islands, Spain) exhibited extreme SWR, with log WDPT ranging from 1.8 to 3.6. SWR has been broadly associated with tree species such as pine due to their hydrophobic substance content (Mataix-Solera et al., 2007).

Lipids, as a hydrophobic substance in plants, were related to CA and log WDPT (Fig. 3). Our result here was similar to the study by Lozano et al. (2013), who found that the increases in lipids content from pine litter induced longer WDPT. In contrast, even though the VA + C. *canephora* mixture had comparable lipids content to other litter sources, it resulted in lower log WDPT. This result might suggest that lipids content alone was insufficient to explain the different WR. Research done by Dao et al. (2022) by physically mixing leaf powder from different plant species with acid-washed sand revealed that WR related to the differences in the concentration and diversity of *n*-alcohols, *n*-fatty acids, and high *n*-alkanes in the leaves. A wider range of plant characteristics may give further insights into which components are primarily responsible for the observed WR.

Our result demonstrates that pH was negatively related to WR, as also shown by some studies (Mataix-Solera et al., 2007; Bonanomi et al., 2016). pH could affect WR by influencing soil microbial and fungi activity. Fungi and other soil microbial activity could induce WR by releasing hydrophobic substances (Doerr et al., 2006; Lozano et al., 2013). Within the pH range of 6 – 9, fungi biomass decreased with higher pH (Rousk et al., 2009). Therefore, it reduced the hydrophobic substances produced by fungi, thus lowering WR. However, we have no empirical data on fungi activity in this experiment. Hence further work

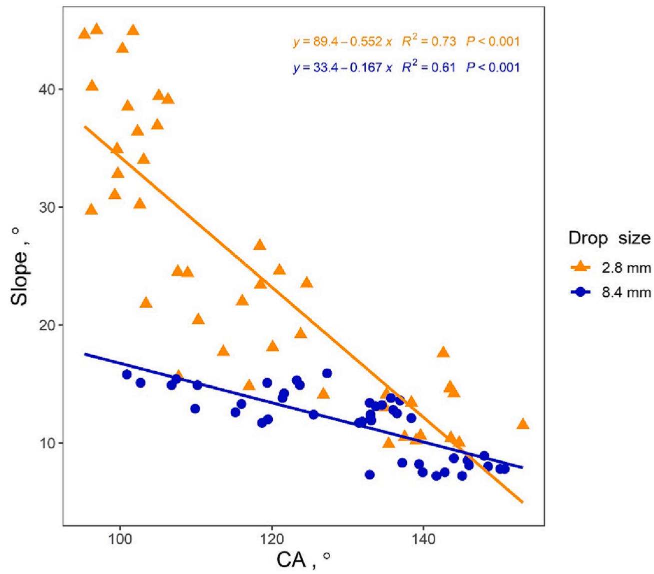

Fig. 5. The relationship between Contact Angle (CA) and critical slope for runoff to start for two different water droplet diameters.

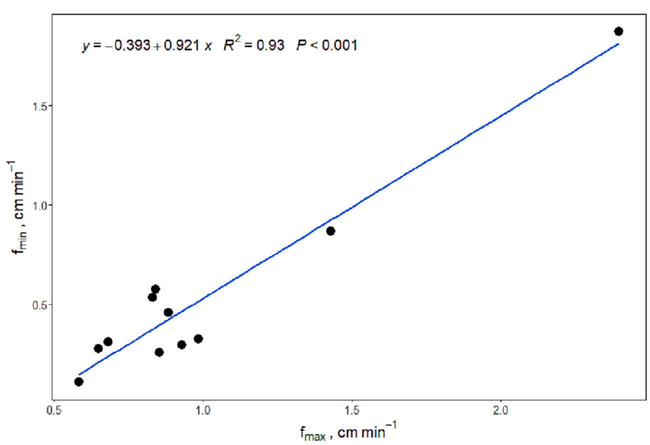

Fig. 6. The initial (f_{max}) and quasi-steady state infiltration rates (f_{min}) estimated from the Horton equation.

is needed. An alternative explanation is linked to soil pH-dependent chemical interaction, such as condensation or hydrolysis as proposed by Smettem et al. (2021). These interactions can lead to the formation or breaking of chemical bonds between organic molecules and soil particles, thus increasing or reducing WR. Furthermore, pH-dependent protonation or deprotonation of phenolic and carboxylic groups, which changes the polarity, have also been found to be correlated with WR (Terashima et al., 2004).

Q2: The critical water content (CWC) and transition zone of water repellent material

The CWC value of the materials in our experiment (10%) was within the range reported by Chau et al. (2014), who found values varying from 0 to > 19% (depending on the specific sample locations), but below the value reported by Doerr and Thomas (2000) with 28%. Meanwhile, the water repellent materials' transition zone in this study was between 0 and 10% water content, corresponding to a 0 to 0.1 $m^3\ m^{-3}$. This range is consistent with the results of several studies, such as Dekker et al. (2001) with a range of 0.02 up to 0.05 $m^3\ m^{-3}$; Leighton-Boyce et al. (2005) with 0.14 to 0.27 $m^3\ m^{-3}$; and Stoof et al. (2011) with 0.18 to 0.41 $m^3\ m^{-3}$.

Knowledge of the CWC and the transition range where soils turn from a hydrophobic to a completely wettable state is valuable, as it provide essential information for remediating or overcoming water-repellent soils. Soil with less persistent WR and lower CWC implies that a large rainfall event may rapidly eliminate the WR. Soil with a high CWC would be prone to preferential flow and runoff due to its lower infiltrability as the soil is persistently hydrophobic at higher water contents. This condition can reduce water storage in the topsoil (Chau et al., 2014). However, once water moves to a greater depth, it may have a longer residence time, as the soil has a slower water movement due to tortuosity of the soil capillary system (Gupta et al., 2015). A hydrophobic soil surface later could also trap the moisture in underlying subsoil layers and provided a barrier to evaporation, which is beneficial during periods of high moisture stress during the dry season (Rye and Smettem, 2017; Smettem et al., 2021).

The emergence of WR in a 'fresh volcanic soil' could be dissimilar to heat exposure-induced WR during a forest fire. In high temperatures during heat exposure, the volatilization and condensation of hydrophobic substances produced from burned organic matter subsequently coated soil particles up to 5 cm below the soil surface, creating a water-repellency layer (DeBano, 1991). The extreme hydrophobic materials could also originate from the fine ash produced after the fire (Bodí et al., 2011; Stoof et al., 2011). Whereas, hydrophobicity in volcanic soils does not always involve heat exposure to organic matter to create WR substances. Coarse-textured VA deposited in agricultural land experiences a cool-down period while drifting in the atmosphere and is not heating the soil when deposited. However, in a particular area close to the eruption epicentre or along the pyroclastic materials flow paths, there is a possibility that organic matter could be exposed to high temperatures and produce hydrophobic substances comparable to forest fire process. In this research, we emphasized the WR formation related to the presence of relatively fine hydrophobic particulate OM in pore space which is directly correlated to the abundance of organic matter in the soil. This specific condition is more or less similar to the non-fire-induced hydrophobic phenomena in sandy soils (Franco et al., 2000; Pierson et al., 2008; Siteur et al., 2016).

Q3: Strong WR properties minimize the critical slope for runoff to start

Dissimilar to the non-water repellent soils, the existence of severe and persistent hydrophobic substances in relatively dry soils and sloping terrain could reduce infiltration and cause fast ponding, thus reducing runoff/erosion generation time. The relationship between WR and the critical slope for the runoff process is essential to predict the runoff/erosion scenarios in different intensities and frequencies of rainfall events.

The minimum critical slope for runoff to start for a large raindrop diameter was 7° (16%). Within our local context, the high rainfall intensity that often occurs in this mountainous area could create a greater risk of runoff and erosion, as the landscape of this region has a slope range from 2 to 40% (Saputra et al., 2022). The temporal variability of runoff generation between non– and water-repellent plots has been found to be highly variable in the short term (early time after the rainfall/irrigation or when the soil water content is still below the CWC). However, as the water content increased beyond CWC and the WR diminished with time, the runoff generation time could become comparable (Pierson et al., 2008). However, at the catchment scale, the overall impact of SWR on runoff, erosion and sedimentation is influenced by the spatial connectivity of the overland flow (runoff) sources areas, as well as the temporary and spatial variability of SWR. This complexity makes it challenging to establish direct links between SWR and erosion (Shakesby et al., 2000). Therefore, a better understanding of the temporal and spatial dynamics of SWR and its interactions with catchment-scale hydrological process is needed to better predict the impacts of SWR on runoff, erosion, and sedimentation.

Q4: Strong water-repellent surface layer reduced infiltration and hydraulic conductivity

Our observed hydraulic conductivity (K_{obs}) values (6–131 cm h^{-1})

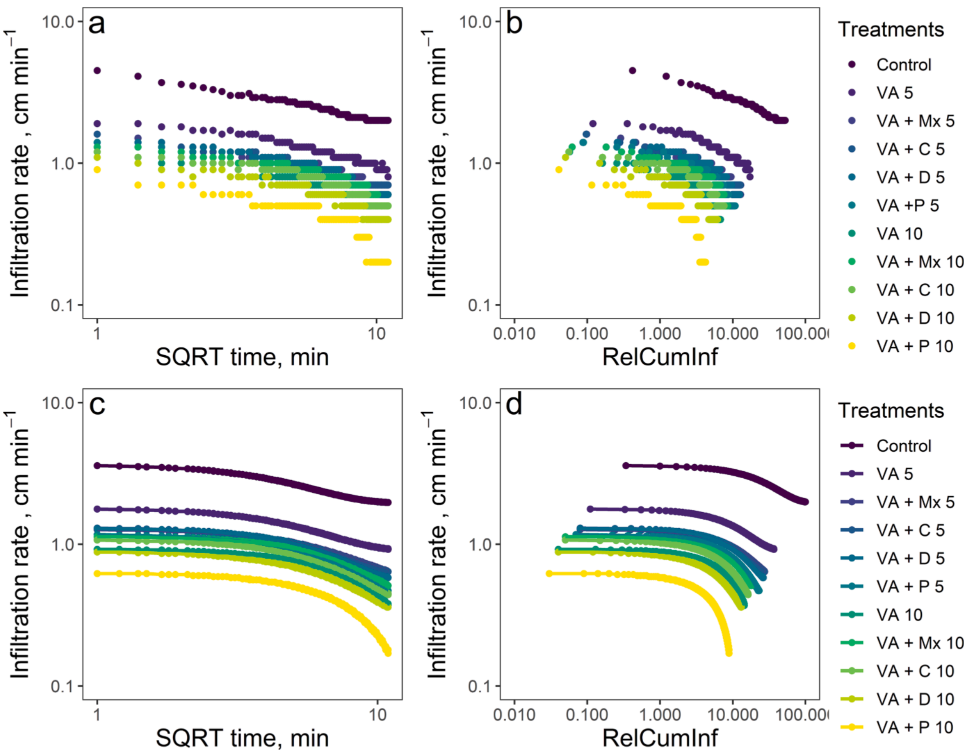

Fig. 7. The infiltration rate as a function of the square root of (SQRT) time (a and c) and cumulative infiltration relative (RelCumInf) to total porosity (b and d). Two upper figures (a and b) were observed data, while two lower figures (c and d) were fitted data using Horton equations. Columns of control soil had 0, 5 or 10 cm of volcanic ash (VA) mixed with different organic matter sources on top. Volcanic ash (VA), VA + organic matter (Mx = mixed quality, C = *C. canephora*, D = *D. zibethinus*, P = *P. merkusii*).

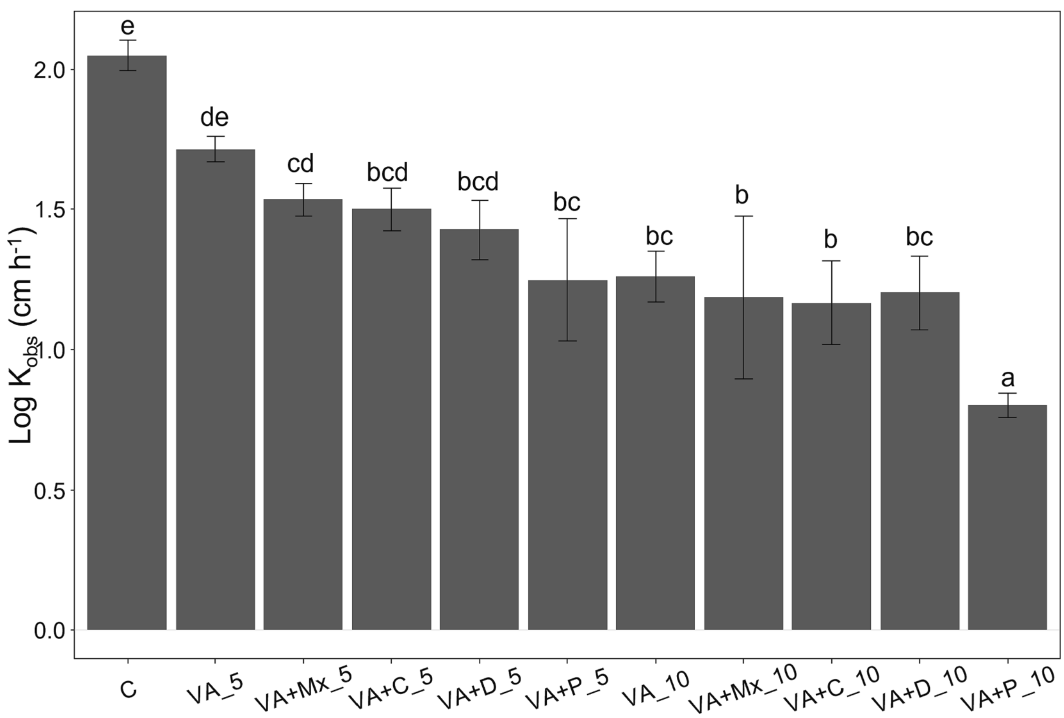

Fig. 8. The observed hydraulic conductivity presented as log K_{obs} (mean ± SE) of two water repellence layers thickness (5 and 10 cm), and six treatments of control/untreated soil (Control), volcanic ash (VA), VA + organic matter (C = *C. canephora*, D = *D. zibethinus*, P = *P. merkusii*, Mx = mixed quality). The different letters indicate statistical differences between treatments ($p \leq 0.05$).

were within the range of sandy soils observed by García-Gutiérrez et al. (2018). Related to WR, our results showed that adding a 5–10 cm layer of hydrophobic material on the soil surface decreased K_{obs} from 69 to 94% (K ratio of 0.31 – 0.06) compared to the K_{ref}. Hydrophobic materials reduce the relative equivalent porosity for the water transmission process in the soil profile (Fig. 9**b**).

We expected that the effect of WR on K_{obs} reduction would be limited to the early phase of the measurement when the water-repellent surface layer was relatively dry. Once the water content of the layer exceeded the CWC, we anticipated that the WR effect would disappear. However, we found that the WR effect on K_{obs} persisted throughout the measurement, rather than being a transient phenomenon in early wetting, as

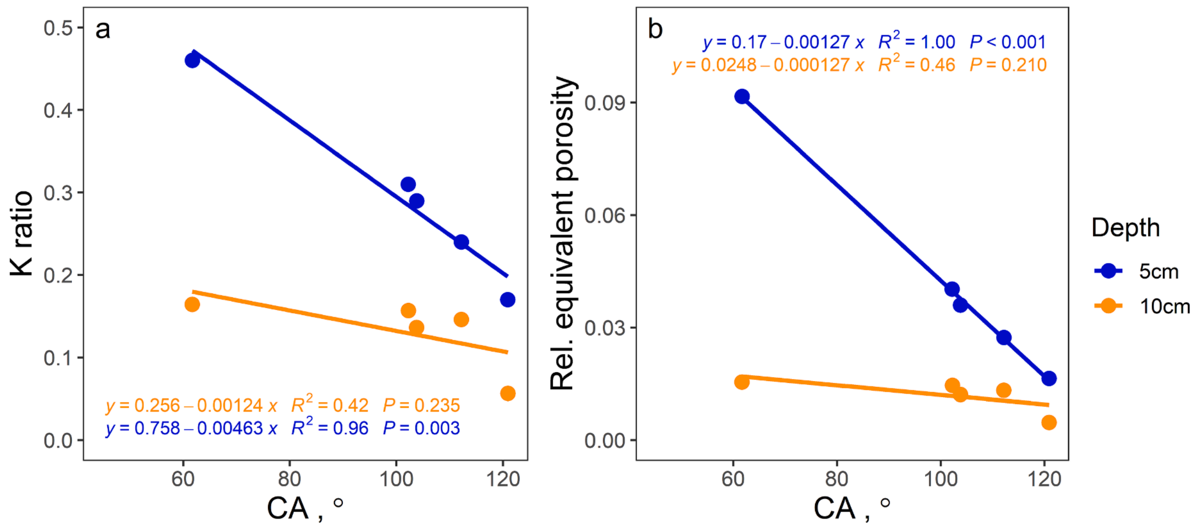

Fig. 9. The relationships between contact angle (CA) and (a) K ratio and (b) relative equivalent porosity on two different water repellence layer thicknesses (5 and 10 cm).

suggested by the effects of soil water content on WDPT.

To interpret these patterns, we propose that air entrapment in soil pores (Faybishenko, 1995) plays a role in hindering the passage of water. It should be noted that the hydraulic conductivity measurements started with the water repellent materials in oven-dried conditions and apparently only partially saturated throughout the measurement. Entrapped air reduces the pore effectiveness to transmit water as it blocks the already limited water pathways (macropores) available in water-repellent material. This effect becomes more pronounced with time as the air bubbles that previously distributed in smaller pores then concentrate in larger pores where water movement mainly occurs, resulting in a sharp decline in infiltration rate in Fig. 7, specifically on the tail section of the infiltration data, and therefore the estimated K_{obs}. At the end, the infiltration rate often slightly increases, but not at the level where it could significantly change K_{sat}, as the air bubbles release to the atmosphere (Concialdi et al., 2019). However, we doubt that we reached this state during this measurement, as we did not observe this pattern from the transient infiltration data (except for the control treatment) in Fig. 7. It is likely because the measurement time was not sufficient for the air bubbles to be fully released.

To quantify the impact of air entrapment on soil infiltration and hydraulic conductivity, Dohnal et al. (2013) used x-ray computed tomography and magnetic resonance imaging combined with three dimensional numerical modelling. Their study indicated that the change of the water flow rate resulted by the air entrapment. Many authors reported that entrapped air could reduce the K_{obs} by 2–20 times compared to air-draining conditions (Faybishenko, 1995; Sakaguchi et al., 2005; Marinas et al., 2013), but this fluctuates depending on the air outflow (Wang et al., 1998). This incomplete saturation of the water-repellent surface layer in the falling head experiments as a plausible reason for decreasing hydraulic conductivity with increasing WR was also previously reported by Shillito et al. (2020). Entrapped air affect the K_{obs} simultaneously with other factors such as soil particle rearrangement and blockage of soil porosity (self-filtration) as reported by Dikinya et al. (2008) that simultaneously. Self-filtration might occur as a consequence of vertical migration of the fine-size water repellent litter, as well as soil particles, during the measurement, and thus naturally lowered the water transmission and hydraulic conductivity. However, we did not find visual evidence of the ash and litter transported to the original soil column after we vertically sliced the soil sample after the measurement. Therefore, further investigation is necessary.

Daily rainfall intensity in East Java, Indonesia peaks at 105–164 mm day^{-1}, with a return period of 5–50 years (Faradiba, 2021). Most rainfall occurs within 1–4 h (Priambodo et al., 2019). Therefore, it is rather likely that water ponding could occur in the field, particularly for the soils which have > 10 cm layer of mixed VA + OM originating from *P. merkusii*, *C. canephora*, and *D. zibethinus* (with an average K_{obs} of 63, 153, and 164 mm h^{-1}, respectively). With the rainfall intensity exceeding infiltration capacity, overland flow could occur in this sloping-mountainous area, despite the high soil macroporosity. However, on days with low rainfall intensity but long duration, entrapped air may easily escape to the soil surface, and WR may be overcome when the soil rewets. Nevertheless, WR will re-emerge when the soil water content is reduced to the transition zone.

WR dynamics on the volcanic landscape

In addition to soil water contents, the dynamics of WR may depend on two other processes: the mobilization of the hydrophobic substances due to soil erosion; and the input (supply) and decomposition rate of hydrophobic substances which is controlled by litter types, microbial activity, and microclimate. Surface runoff is likely to carry the soil materials (including the hydrophobic substances) within the steep slope area and might be deposited in the valley or a relatively flat area. However, the WR effect in the valley area may not be as apparent as in the upper part of the landscape, as the valley area usually has high water content (which is likely to exceed the CWC of this particular area).

Furthermore, it is commonly acknowledged that hydrophobic substances come from the non-polar aliphatic hydrocarbons and polar amphiphilic hydrocarbons groups derived from OM (Doerr et al., 2000). Therefore, further decomposition of OM and its hydrophobic substances contained therein, which is controlled by the soil organisms' (decomposer) activity, could lead to a decrease in WR. However, as an OM decomposer, the presence of fungi and other microorganisms may also induce WR (Doerr et al., 2006; Lozano et al., 2013). However, the long-term net effect depends on the standing OM content, determined by its input and decomposition rate balance. The dynamics of soil organic matter are influenced by vegetation types (quality and quantity OM), microclimate conditions (temperature and water content), and the activity of soil microorganisms (decomposers) (Sari et al., 2022). Post-volcanic eruption soil management by farmers in the study area, such as adding a significant amount of external organic matter and mixing it with volcanic ash and the underlying original soil appears to accelerate soil recovery (Ishaq et al., 2020). However, this practice may also have an adverse effect by inducing WR of the soil surface.

WR implications on landscape modification and its ecological functions

At the plot and landscape scale, the development of WR contributed to VA distribution. VA was not only transported to the landscape directly during the volcanic eruption via the atmosphere, but also through further movement from the runoff and erosion process due to the low infiltration. The potential negative impact of WR on the landscape level could be costly, for example, when it is associated with river/water reservoir sedimentation and water quality. Heavy sedimentation of volcanic materials in the water reservoir could disrupt the electricity supply, generate eutrophication, and cause irrigation water shortages. On the other hand, WR established in volcanic soils could also have positive effect on soil moisture conservation against evaporative loss, facilitate groundwater recharge, and replenishment of deep moisture storage (Lozano et al., 2013; Gupta et al., 2015; Rye and Smettem, 2017; Smettem et al., 2021).

5. Conclusions

It is concluded that adding various litter sources to volcanic ash at a range of soil water contents affects the WR dynamics during a 16-weeks incubation period. Stronger WR was partially associated with higher lipids content and lower pH, indicating another possible influencing factor related to OM composition. The lower WR was directly controlled by the water content rather than changes in lipids and pH, particularly at water treatments > 7%. Additionally, we found that the minimum critical slope for droplets to runoff (before infiltration) was 7° and 10° for large and small water droplet diameters, respectively. Finally, the addition of volcanic ash and litter on the surface of the control soil resulted in a five-times lower average hydraulic conductivity due to the combined effect of soil WR and entrapped air in the soil column. This combination effect led to the effective porosity reduction to transmit water, with 10 cm of layer addition showing the largest effect.

The WR phenomena in relatively young volcanic soils likely contribute to shaping volcanic landscapes. Despite the negative short-term consequences, volcanic ash might benefit soil moisture conservation, nutrient addition, and potential carbon sequestration in soils. Therefore, further research on optimising the benefit and reducing the adverse effects of volcanic ash through land use management is needed.

Declaration of Competing Interest

The authors declare that they have no known competing financial interests or personal relationships that could have appeared to influence the work reported in this paper.

Data availability

Data will be made available on request.

Acknowledgements

We acknowledge the support from M. Rizky Maulana Ishaq from The Department of Soil Science and Forestry, Brawijaya University, for his field assistance. We appreciated the comments from Dr Tom Schut from Plant Production Systems Group, and Dr Marius Heinen from Team Soil, Water and Land Use, Wageningen University and Research on the earlier draft, and thank three anonymous reviewers for corrections, clarifying questions, and suggestions.

Funding

This work was supported by the Ministry of Finance, the Republic of Indonesia, through the BUDI LN scholarships scheme coordinated by the Indonesia Endowment Fund for Education (LPDP).

Author contributions

All authors contributed to the study's conception, plan and design. DDS and INS conducted the material preparation, lab work and lab analysis. DDS, RRS, and MvN analysed the data. DDS and MvN wrote the first draft of the manuscript and all authors commented on previous versions of the manuscript. All authors have read and approved the final manuscript.

Appendix A. Supplementary data

Supplementary data to this article can be found online at https://doi.org/10.1016/j.geoderma.2023.116535.

References

Anda, M., Suparto, S., 2016. Characteristics of pristine volcanic materials: beneficial and harmful effects and their management for restoration of agroecosystem. Sci. Total Environ. 543, 480–492. https://doi.org/10.1016/j.scitotenv.2015.10.157.

Anderson, J., Ingram, J., 1994. Tropical Soil Biology and Fertility: A Handbook of Methods. Soil Sci. 157, 265. https://www.jstor.org/stable/2261129.

Arnalds, O., 2013. The influence of volcanic tephra (Ash) on ecosystems. Adv. Agron. 121, 331–380. https://doi.org/10.1016/B978-0-12-407685-3.00006-2.

Bachmann, J., Ellies, A., Hartge, K.H., 2000. Development and application of a new sessile drop contact angle method to assess soil water repellency. J. Hydrol. 231–232, 66–75. https://doi.org/10.1016/S0022-1694(00)00184-0.

Baker, S.W., 1979. Pore size distribution — A factor to be considered in infiltration studies? Journal of Hydrology 41, 279–290. https://doi.org/10.1016/0022-1694(79)90066-0.

Berenstecher, P., Gangi, D., González-Arzac, A., Martínez, M.L., Chaves, E.J., Mondino, E. A., Austin, A.T., Treseder, K., 2017. Litter microbial and soil faunal communities stimulated in the wake of a volcanic eruption in a semi-arid woodland in Patagonia, Argentina. Funct. Ecol. 31 (1), 245–259.

Bieganowski, A., Ryżak, M., 2011. Soil texture: measurement methods. In: Gliński, J., Horabik, J., Lipiec, J. (Eds.), Encyclopedia of Agrophysics. Springer, Netherlands, Dordrecht, pp. 791–794. https://doi.org/10.1007/978-90-481-3585-1_157.

Bisdom, E.B.A., Dekker, L.W., Schoute, J.F.T., 1993. Water repellency of sieve fractions from sandy soils and relationships with organic material and soil structure. Geoderma 56, 105–118. https://doi.org/10.1016/0016-7061(93)90103-R.

Bodí, M.B., Mataix-Solera, J., Doerr, S.H., Cerdà, A., 2011. The wettability of ash from burned vegetation and its relationship to Mediterranean plant species type, burn severity and total organic carbon content. Geoderma 160, 599–607. https://doi.org/10.1016/j.geoderma.2010.11.009.

Bonanomi, G., Gaglione, S.A., Antignani, V., Cesarano, G., 2016. Unimodal pattern of soil hydrophobicity along an altitudinal gradient encompassing Mediterranean, temperate, and alpine ecosystems. Plant Soil 409, 37–47. https://doi.org/10.1007/s11104-016-3020-0.

Chae, H.M., Choi, S.H., Lee, S.H., Cha, S., Yang, K.C., Shim, J.K., 2019. Effect of litter quality on needle decomposition for four pine species in Korea. Forests 10 (5), 371.

Chau, H.W., Biswas, A., Vujanovic, V., Si, B.C., 2014. Relationship between the severity, persistence of soil water repellency and the critical soil water content in water repellent soils. Geoderma 221–222, 113–120. https://doi.org/10.1016/j.geoderma.2013.12.025.

Concialdi, P., Bagarello, V., Alagna, V., Iovino, M., 2019. Laboratory evaluation of falling-head infiltration for saturated soil hydraulic conductivity determination. J. Agric. Eng. 51, 27–35. https://doi.org/10.4081/jae.2019.1003.

Dao, M.T.T., Henry, D.J., Dell, B., Daniel, N.R.R., Harper, R.J., 2022. Induction of water repellency by leaves of contrasting Australian native species: effects of composition and heating. Plant and Soil 478, 505–517. https://doi.org/10.1007/s11104-022-05492-4.

de Blas, E., Almendros, G., Sanz, J., 2013. Molecular characterization of lipid fractions from extremely water-repellent pine and eucalyptus forest soils. Geoderma 206, 75–84. https://doi.org/10.1016/j.geoderma.2013.04.027.

DeBano, L.F., 1991. The effect of fire on soil properties. In: Harvey, Alan E.; Neuenschwander, Leon F., compilers. Proceedings-management and productivity of western-montane forest soils; 1990 April 10-12; Boise, ID. Gen. Tech. Rep. INT-280. Ogden, UT: U.S. Department of Agriculture, Forest Service, Intermountain Research Station. p. 151-156. Access date: 25 February 2022. Available at: https://www.fs.usda.gov/treesearch/pubs/42163.

Dekker, L.W., Doerr, S.H., Oostindie, K., Ziogas, A.K., Ritsema, C.J., 2001. Water repellency and critical soil water content in a dune sand. Soil Sci. Soc. Am. J. 65, 1667–1674. https://doi.org/10.2136/sssaj2001.1667.

Dikinya, O., Hinz, C., Aylmore, G., 2008. Decrease in hydraulic conductivity and particle release associated with self-filtration in saturated soil columns. Geoderma 146, 192–200. https://doi.org/10.1016/j.geoderma.2008.05.014.

Doerr, S.H., Shakesby, R.A., Walsh, R.P.D., 2000. Soil water repellency: its causes, characteristics and hydro-geomorphological significance. Earth Sci. Rev. 51, 33–65. https://doi.org/10.1016/S0012-8252(00)00011-8.

Doerr, S.H., Llewellyn, C.T., Douglas, P., Morley, C.P., Mainwaring, K.A., Haskins, C., Johnsey, L., Ritsema, C.J., Stagnitti, F., Allinson, G., Ferreira, D., Keizer, J.J., Ziogas, A.K., Diamantis, J., 2005. Extraction of compounds associated with water repellency in sandy soils of different origin. Soil Res. 43 (3), 225.

Doerr, S.H., Shakesby, R.A., Dekker, L.W., Ritsema, C.J., 2006. Occurrence, prediction and hydrological effects of water repellency amongst major soil and land-use types in a humid temperate climate. Eur. J. Soil Sci. 57, 741–754. https://doi.org/10.1111/j.1365-2389.2006.00818.x.

Doerr, S.H., Thomas, A.D., 2000. The role of soil moisture in controlling water repellency: new evidence from forest soils in Portugal. J. Hydrol. 231–232, 134–147. https://doi.org/10.1016/S0022-1694(00)00190-6.

M. Dohnal V. Jelinkova M. Snehota J. Dusek J. Brezina Tree-Dimensional Numerical Analysis of Water Flow Affected by Entrapped Air: Application of Noninvasive Imaging Techniques Vadose Zone Journal 12 1 2013 10.2136/vzj2012.0078 vzj2012.0078.

Ellerbrock, R.H., Gerke, H.H., Bachmann, J., Goebel, M.-O., 2005. Composition of organic matter fractions for explaining wettability of three forest soils. Soil Sci. Soc. Am. J. 69, 57–66. https://doi.org/10.2136/sssaj2005.0057.

Faradiba, 2021. Analysis of intensity, duration, and frequency rain daily of java island using mononobe method. J. Phys. Conf. Ser. 1783, 012107 https://doi.org/10.1088/1742-6596/1783/1/012107.

Faybishenko, B.A., 1995. Hydraulic behavior of quasi-saturated soils in the presence of entrapped air: laboratory experiments. Water Resour. Res. 31, 2421–2435. https://doi.org/10.1029/95WR01654.

Franco, C.M.M., Clarke, P.J., Tate, M.E., Oades, J.M., 2000. Hydrophobic properties and chemical characterisation of natural water repellent materials in Australian sands. J. Hydrol. 231–232, 47–58. https://doi.org/10.1016/S0022-1694(00)00182-7.

García-Gutiérrez, C., Pachepsky, Y., Martín, M.Á., 2018. Technical note: Saturated hydraulic conductivity and textural heterogeneity of soils. Hydrol. Earth Syst. Sci. 22, 3923–3932. https://doi.org/10.5194/hess-22-3923-2018.

Gupta, B., Shah, D.O., Mishra, B., Joshi, P.A., Gandhi, V.G., Fougat, R.S., 2015. Effect of top soil wettability on water evaporation and plant growth. J. Colloid Interface Sci. 449, 506–513.

Hammecker, C., Antonino, A.C.D., Maeght, J.L., Boivin, P., 2003. Experimental and numerical study of water flow in soil under irrigation in northern Senegal: evidence of air entrapment. Eur. J. Soil Sci. 54, 491–503. https://doi.org/10.1046/j.1365-2389.2003.00482.x.

Helrich, K., 1990. Official methods of analysis of the Association of Official Analytical Chemists. Association of official analytical chemists. Access date: 03 March 2022. Available at: https://law.resource.org/pub/us/cfr/ibr/002/aoac.methods.1.1990.pdf.

Hidayat, F., Juwono, P.T., Suharyanto, A., Pujiraharjo, A., Legono, D., Sisinggih, D., Neil, D., Fujita, M., Sumi, T., 2017. Assessment of sedimentation in wlingi and lodoyo reservoirs: a secondary disaster following the 2014 Eruption of Mt Kelud, Indonesia. J. Disaster Res. 12 (3), 617–630. https://doi.org/10.20965/jdr.2017.p0617.

Hodnett, M.G., Tomasella, J., 2002. Marked differences between van Genuchten soil water-retention parameters for temperate and tropical soils: a new water-retention pedo-transfer functions developed for tropical soils. Geoderma 108, 155–180. https://doi.org/10.1016/S0016-7061(02)00105-2.

Horton, R.E., 1941. An approach toward a physical interpretation of infiltration-capacity. Soil Sci. Soc. Am. J. 5, 399–417. https://doi.org/10.2136/sssaj1941.036159950005000C0075x.

Husson, O., 2013. Redox potential (Eh) and pH as drivers of soil/plant/microorganism systems: a transdisciplinary overview pointing to integrative opportunities for agronomy. Plant Soil 362, 389–417. https://doi.org/10.1007/s11104-012-1429-7.

Ishaq, R.M., Saputra, D.D., Sari, R.R., Suprayogo, D., Widianto, W., Prayogo, C., Hairiah, K., 2020. Turning volcanic ash into fertile soil: farmers' options in coffee agroforestry after the 2014 mount Kelud Eruption. AGRIVITA. J. Agric. Sci. 42 (1).

Jenkins, S., Komorowski, J.-C., Baxter, P.J., Spence, R., Picquout, A., Lavigne, F., Surono, 2013. The Merapi 2010 eruption: an interdisciplinary impact assessment methodology for studying pyroclastic density current dynamics. J. Volcanol. Geoth. Res. 261, 316–329.

Jiménez-Morillo, N.T., Spangenberg, J.E., Miller, A.Z., Jordán, A., Zavala, L.M., González-Vila, F.J., González-Pérez, J.A., 2017. Wildfire effects on lipid composition and hydrophobicity of bulk soil and soil size fractions under Quercus suber cover (SW-Spain). Environ Res. 159, 394–405.

Jordán, A., Zavala, L.M., Nava, A.L., Alanís, N., 2009. Occurrence and hydrological effects of water repellency in different soil and land use types in Mexican volcanic highlands. Catena 79, 60–71. https://doi.org/10.1016/j.catena.2009.05.013.

Jordán, A., Zavala, L.M., Mataix-Solera, J., Nava, A.L., Alanís, N., 2011. Effect of fire severity on water repellency and aggregate stability on Mexican volcanic soils. Catena 84, 136–147. https://doi.org/10.1016/j.catena.2010.10.007.

Kawamoto, K., Moldrup, P., Komatsu, T., De Jonge, L.W., Oda, M., 2007. Water repellency of aggregate size fractions of a volcanic ash soil. Soil Sci. Soc. Am. J. 71, 1658–1666. https://doi.org/10.2136/sssaj2006.0284.

Korup, O., Seidemann, J., Mohr, C.H., 2019. Increased landslide activity on forested hillslopes following two recent volcanic eruptions in Chile. Nat. Geosci. 12, 284–289. https://doi.org/10.1038/s41561-019-0315-9.

Lavigne, F., 2004. Rate of sediment yield following small-scale volcanic eruptions: a quantitative assessment at the Merapi and Semeru stratovolcanoes, Java, Indonesia. Earth Surf. Proc. Land. 29, 1045–1058. https://doi.org/10.1002/esp.1092.

Leelamanie, D.A.L., Karube, J., Yoshida, A., 2008. Characterizing water repellency indices: Contact angle and water drop penetration time of hydrophobized sand. Soil Sci. Plant Nutr. 54, 179–187. https://doi.org/10.1111/j.1747-0765.2007.00232.x.

Leighton-Boyce, G., Doerr, S.H., Shakesby, R.A., Walsh, R.P.D., Ferreira, A.J.D., Boulet, A.-K., Coelho, C.O.A., 2005. Temporal dynamics of water repellency and soil moisture in eucalypt plantations, Portugal. Soil Res. 43 (3), 269.

Lozano, E., Jiménez-Pinilla, P., Mataix-Solera, J., Arcenegui, V., Bárcenas, G.M., González-Pérez, J.A., García-Orenes, F., Torres, M.P., Mataix-Beneyto, J., 2013. Biological and chemical factors controlling the patchy distribution of soil water repellency among plant species in a Mediterranean semiarid forest. Geoderma 207-208, 212–220.

Lucas-Borja, M.E., Fernández, C., Plaza-Alvarez, P.A., Zema, D.A., 2022. Variability of hydraulic conductivity and water repellency of soils with fire severity in pine forests and reforested areas under Mediterranean conditions. Ecohydrology 15, e2472.

Mahapatra, S., Jha, M.K., Biswal, S., Senapati, D., 2020. Assessing Variability of Infiltration Characteristics and Reliability of Infiltration Models in a Tropical Sub-humid Region of India. Sci. Rep. 10, 1515. https://doi.org/10.1038/s41598-020-58333-8.

Marinas, M., Roy, J.W., Smith, J.E., 2013. Changes in entrapped gas content and hydraulic conductivity with pressure. Groundwater 51, 41–50. https://doi.org/10.1111/j.1745-6584.2012.00915.x.

Mataix-Solera, J., Arcenegui, V., Guerrero, C., Mayoral, A.M., Morales, J., González, J., García-Orenes, F., Gómez, I., 2007. Water repellency under different plant species in a calcareous forest soil in a semiarid Mediterranean environment. Hydrol. Process. 21 (17), 2300–2309.

Nakada, S., Zaennudin, A., Maeno, F., Yoshimoto, M., Hokanishi, N., 2016. Credibility of volcanic ash thicknesses reported by the media and local residents following the 2014 Eruption of Kelud Volcano, Indonesia. J. Disaster Res. 11 (1), 53–59.

Neris, J., Jiménez, C., Fuentes, J., Morillas, G., Tejedor, M., 2012. Vegetation and land-use effects on soil properties and water infiltration of Andisols in Tenerife (Canary Islands, Spain). Catena 98, 55–62. https://doi.org/10.1016/j.catena.2012.06.006.

Neris, J., Tejedor, M., Rodríguez, M., Fuentes, J., Jiménez, C., 2013. Effect of forest floor characteristics on water repellency, infiltration, runoff and soil loss in Andisols of Tenerife (Canary Islands, Spain). Catena 108, 50–57. https://doi.org/10.1016/j.catena.2012.04.011.

Novák, V., Lichner, Ľ., Zhang, B., Kňava, K., 2009. The impact of heating on the hydraulic properties of soils sampled under different plant cover. Biologia 64, 483–486. https://doi.org/10.2478/s11756-009-0099-2.

Pensa, A., Capra, L., Giordano, G., 2019. Ash clouds temperature estimation. Implication on dilute and concentrated PDCs coupling and topography confinement. Sci. Rep. 9, 5657. https://doi.org/10.1038/s41598-019-42035-x.

Perera, C., Brown, R.H., 1996. A new method for lipid extraction at ambient temperature. Cienc. Tecnol. Aliment. 1, 13–18. https://doi.org/10.1080/11358129609487557.

Pierson, T.C., Major, J.J., 2014. Hydrogeomorphic effects of explosive volcanic eruptions on drainage basins. Annu. Rev. Earth Planet. Sci. 42, 469–507. https://doi.org/10.1146/annurev-earth-060313-054913.

Pierson, F.B., Robichaud, P.R., Moffet, C.A., Spaeth, K.E., Williams, C.J., Hardegree, S.P., Clark, P.E., 2008. Soil water repellency and infiltration in coarse-textured soils of burned and unburned sagebrush ecosystems. Catena 74 (2), 98–108.

Poulenard, J., Michel, J.C., Bartoli, F., Portal, J.M., Podwojewski, P., 2004. Water repellency of volcanic ash soils from Ecuadorian páramo: Effect of water content and characteristics of hydrophobic organic matter. Eur. J. Soil Sci. 55, 487–496. https://doi.org/10.1111/j.1365-2389.2004.00625.x.

Priambodo, S., Suhardjono, L., Suhartanto, E., 2019. Hourly rainfall distribution patterns in Java island. MATEC Web of Conferences. https://doi.org/10.1051/matecconf/201927604012.

Purwanto, Baon, J.B., Hairiah, K., 2007. Kualitas Masukan Seresah Pohon Penaung Dapat Menjadi Regulator Nitrifikasi Pada Lahan Agroforestri Kopi. Pelita Perkebunan 23, 183–204. http://perkebunan.litbang.pertanian.go.id/dbasebun/asset_dbasebun/Penerbitan-20141207120521.pdf.

R Core Team, 2021. R: A language and environment for statistical computing. R Foundation for Statistical Computing, Vienna, Austria.

Rossi, E., Bagheri, G., Beckett, F., Bonadonna, C., 2021. The fate of volcanic ash: premature or delayed sedimentation? Nat. Commun. 12, 1303. https://doi.org/10.1038/s41467-021-21568-8.

Rousk, J., Brookes Philip, C., Bååth, E., 2009. Contrasting Soil pH Effects on Fungal and Bacterial Growth Suggest Functional Redundancy in Carbon Mineralization. Appl. Environ. Microbiol. 75, 1589–1596. https://doi.org/10.1128/AEM.02775-08.

Rye, C.F., Smettem, K.R.J., 2017. The effect of water repellent soil surface layers on preferential flow and bare soil evaporation. Geoderma 289, 142–149. https://doi.org/10.1016/j.geoderma.2016.11.032.

Sakaguchi, A., Nishimura, T., Kato, M., 2005. The effect of entrapped air on the quasi-saturated soil hydraulic conductivity and comparison with the Unsaturated Hydraulic Conductivity. Vadose Zone J. 4, 139–144. https://doi.org/10.2136/vzj2005.0139.

Saputra, D.D., Sari, R.R., Hairiah, K., Roshetko, J.M., Suprayogo, D., van Noordwijk, M., 2020. Can cocoa agroforestry restore degraded soil structure following conversion from forest to agricultural use? Agrofor. Syst. 94 (6), 2261–2276.

Saputra, D.D., Sari, R.R., Hairiah, K., Widianto, Suprayogo, D., van Noordwijk, M., 2022. Recovery after volcanic ash deposition: vegetation effects on soil organic carbon, soil structure and infiltration rates. Plant Soil 474 (1-2), 163–179.

Sari, R.R., Rozendaal, D.M.A., Saputra, D.D., Hairiah, K., Roshetko, J.M., van Noordwijk, M., 2022. Balancing litterfall and decomposition in cacao agroforestry systems. Plant Soil 473 (1-2), 251–271.

Shakesby, R.A., Doerr, S.H., Walsh, R.P.D., 2000. The erosional impact of soil hydrophobicity: current problems and future research directions. J. Hydrol. 231–232, 178–191. https://doi.org/10.1016/S0022-1694(00)00193-1.

Shillito, R.M., Berli, M., Ghezzehei, T.A., 2020. Quantifying the effect of subcritical water repellency on sorptivity: a physically based model. Water Resour. Res. 56 https://doi.org/10.1029/2020WR027942 e2020WR027942.

Simpson, J.T., Hunter, S.R., Aytug, T., 2015. Superhydrophobic materials and coatings: a review. Rep. Prog. Phys. 78 (8), 086501.

Siteur, K., Mao, J., Nierop, K.G.J., Rietkerk, M., Dekker, S.C., Eppinga, M.B., 2016. Soil water repellency: a potential driver of vegetation dynamics in coastal dunes. Ecosystems 19 (7), 1210–1224.

Smettem, K.R.J., Rye, C., Henry, D.J., Sochacki, S.J., Harper, R.J., 2021. Soil water repellency and the five spheres of influence: a review of mechanisms, measurement and ecological implications. Sci. Total Environ. 787, 147429 https://doi.org/10.1016/j.scitotenv.2021.147429.

Stadler, A., Sage, D., 2020. Drop Shape Analysis, Biomedical Imaging Group. Access date: 04 March 2022. Available at: http://bigwww.epfl.ch/demo/dropanalysis/.

Stoof, C.R., Moore, D., Ritsema, C.J., Dekker, L.W., 2011. Natural and fire-induced soil water repellency in a Portuguese shrubland. Soil Sci. Soc. Am. J. 75, 2283–2295. https://doi.org/10.2136/sssaj2011.0046.

Tarasenko, I., Bielders, C., Guevara, A., Delmelle, P., 2019. Surface crusting of volcanic ash deposits under simulated rainfall. Bull. Volcanol. 81 https://doi.org/10.1007/s00445-019-1289-6.

Tejedor, M., Neris, J., Jiménez, C., 2013. Soil Properties Controlling Infiltration in Volcanic Soils (Tenerife, Spain). Soil Science Society of America Journal 77, 202–212. https://doi.org/10.2136/sssaj2012.0132.

Terashima, M., Fukushima, M., Tanaka, S., 2004. Influence of pH on the surface activity of humic acid: micelle-like aggregate formation and interfacial adsorption. Colloids Surf. A Physicochem. Eng. Asp. 247, 77–83. https://doi.org/10.1016/j.colsurfa.2004.08.028.

Wang, Z., Feyen, J., van Genuchten, M.T., Nielsen, D.R., 1998. Air entrapment effects on infiltration rate and flow instability. Water Resour. Res. 34, 213–222. https://doi.org/10.1029/97WR02804.

Wang, Z., Wu, Q.J., Wu, L., Ritsema, C.J., Dekker, L.W., Feyen, J., 2000. Effects of soil water repellency on infiltration rate and flow instability. J. Hydrol. 231-232, 265–276.

Wilson, T., Cole, J., Cronin, S., Stewart, C., Johnston, D., 2011. Impacts on agriculture following the 1991 eruption of Vulcan Hudson, Patagonia: lessons for recovery. Nat. Hazards 57, 185–212. https://doi.org/10.1007/s11069-010-9604-8.

Yakubu, M.L., Yusop, Z., Fulazzaky, M.A., 2016. The influence of rain intensity on raindrop diameter and the kinetics of tropical rainfall: case study of Skudai, Malaysia. Hydrol. Sci. J. 61, 944–951. https://doi.org/10.1080/02626667.2014.934251.

Zehetner, F., Miller, W.P., 2006. Erodibility and runoff-infiltration characteristics of volcanic ash soils along an altitudinal climosequence in the Ecuadorian Andes. Catena 65, 201–213. https://doi.org/10.1016/j.catena.2005.10.003.